UNIVERSITY OF PIRAEUS

DEPARTMENT OF DIGITAL SYSTEMS

POLARIZED MIMO OVER SATELLITE

Master Thesis

PETROPOULOU PARASKEVI

ME/10070

ppetrop@unipi.com

SUPERVISOR

Professor ATHANASIOS G. KANATAS

this thesis is dedicated to my parents

and my brother

Acknowledgements

My sincere thanks to Professor Athanasios Kanatas who not only is a remarkable person aside his talented teaching skills, but also for guiding, motivating and supporting me throughout my entire academic path.

I also want to pay my respects to all the professors and lectures of the Postgraduate Program for being more than willing to share their knowledge and assist us through any way possible.

It goes without saying that without my family's psychological and economical support I would not have made it to here. All my achievements are dedicated to them.

Lastly, I want to thank my closest friends for putting up with me and stand by me all those years especially in stressful times and times of hard work.

Abstract

THE present dissertation addresses to the subject of polarization implementation to MIMO satellite communication systems. It is a known fact that due to lack of scatterers near the transmitter (satellite) and space restrictions on the transmitter, a strong LoS is more often than not present, resulting in a very high channel correlation which, in turn, does not permit the creation of independent propagation paths. A very promising solution to alleviate, if not solve, the above described issue is the use of polarization techniques which are in place to offer additional degrees of freedom for exploitation.

Only in recent years has polarization started to draw attention as a research subject. A plethora of surveys have been conducted since then, gathering results and information referring to terrestrial and satellite communication systems for indoor and outdoor environments, revealing that polarization have the prospect to be considered as a very useful and versatile tool.

This thesis after building step by step all the needed theoretic background referring to wave propagation, propagation mechanisms, etc., concludes with the description of a Polarized 2x2 MIMO Land Mobile Satellite communications system model. The simulation of the system model follows with results for the system's performance including BER, XPD and capacity.

Table of Contents

Table of Figures

Abbreviations

3GPP /2	3rd Generation Partnership Project /2
BER	Bit Error Rate
BS(s)	Base Station(s)
DVB-SH	Digital Video Broadcasting - Satellite services to Handhelds
DVB-NGH	Digital Video Broadcasting - Next Generation Handheld
FS	Fixed Satellite
FSL	Free Space Loss
IEEE	Institute of Electrical and Electronics Engineers
ITU	International Telecommunication Union
LD	Linear Detector
LHCP	Left Hand Circular Polarization
LMS	Land Mobile channel
LoS	Line of Sight
MIMO	Multiple-Input Multiple-Output
MIMO-MU	MIMO MultiUser
MISO	Multiple Input Single Output
MMSE	Minimum Mean Square Error
MST	Mobile Satellite Terminal
MS	Mobile Satelite
NGN	Next Generation Network
NLoS	Non Line of Sight
OSIC	Ordered Successive Interference Cancellation

RHCP	Right Hand Circular Polarization
QoS	Quality of Service
SatCom(s)	SATellite COMmunication(s)
SIC-MMSE	Successive Interference Cancellation- Minimum Mean Square Error
SIC-ZF	Successive Interference Cancellation- Zero Forcing
SIMO	Single Input Multiple Output
SINR	Signal-to-Interference-plus-Noise Ratio
SISO	Single Input Single Output
SM	Spatial Multiplexing
SNR	Signal to Noise Ratio
ZF	Zero forcing
VHF	Very High Frequency
XPC	Cross Polarization Coupling
XPD	Cross Polarization Discrimination
XPI	Cross Polarization Isolation

1. Introduction

1.1. An Overview of Wireless Communications

IT is well known that one of the most important human primitive characteristics is the need for communication. We live in the century where technology, in general, is gaining more ground than ever in our everyday lives. Wireless communications are becoming more and more of an integral part in our daily activities from the simple act of using a cellphone to make a call or seeing a movie on satellite television, to communicating and exchanging data with everyone owning a smartphone or a computer on every corner around the world. Whereas in the early days of mobile communications Quality of Service (QoS) was often poor, nowadays it is assumed the service will be ubiquitous, of high speech quality so for example, the ability to watch and share streaming video is forcing providers to offer even higher uplink and downlink data-rates, whilst maintaining an appropriate QoS.

Terrestrial mobile communications infrastructure has made deep inroads around the world. While most rural areas are obtaining good coverage in many countries, there are still geographically remote and isolated places without good coverage, and worst, there are towns and/or large cities with no coverage at all. To counteract this phenomenon, satellite mobile communications are in place to offer the benefit of true global coverage, reaching into the most secluded areas as well as populated areas, so the rapid deployment of satellite networks, which strongly support terrestrial backbone networks and provide extensive and uninterrupted radio coverage to stationary, portable, and mobile terrestrial receivers seems the only way towards a universal coverage [1], [2]. This has made them very popular for niche markets like news reporting, military and disaster relief services. However, until now there has been no wide-ranging adoption of mobile satellite communications to the mass market.

In addition, satellite based mobile communications offer great advantages in delivering multicast and broadcast traffic because of their intrinsic broadcast nature. The utilization of satellites to complement terrestrial mobile communications for bringing this type of traffic to the mass market is gaining increasing support in the standards groups, as it may well be the cheapest and most efficient method of doing so. Current mobile satellite communication systems however often suffer from poorer QoS due to high path loss, shadowing, blockage, limited satellite power and high link delay. Unfortunately, even with state of the art high power satellites with narrow spot beams or multiple satellite constellations, link availability is not always possible when the signal is blocked by buildings, not to mention indoor coverage where more often than not is unacceptable. With future satellites providing substantially more radiated power and possibly using diversity techniques, users may someday perceive the same QoS from a satellite based mobile communication. It is needless to say that there is a long way to go before this is achieved. Satellite communication system operators are always trying to achieve adequate QoS with the minimum fade margin (and therefore cost) [3]. However, signal blockage can easily be 30dB or more, and the link would be dropped. Even with multiple satellites offering satellite diversity, signal availability is not guaranteed. Along with the described issue, day by day, new requirements are emerging for greater bandwidth, higher data rates, and improved QoS [4], [5].

The implementation of Multiple-Input Multiple-Output (MIMO) systems, where more than one antenna is available at each end of the communication link, has become a highly researched area since ground-breaking work during the nineties showed that large increases in capacity over the Shannon limit were available without increase in power or bandwidth. The MIMO technology has played an important role in significantly revolutionizing the terrestrial wireless networks leading to growing acknowledgement from the research community, industry, and wireless standardization bodies, e.g., IEEE 802, 3GPP/3GPP2 and WINNER projects. The core idea behind MIMO technology is the use of space-time processing in which time is complemented with the spatial dimension inherent in the use of multiple spatially distributed antennas. Some improvements to land mobile satellite (LMS)

communication systems are available by using this technique of satellite-MIMO between the satellite and mobile in both directions.

To remain competitive with the terrestrial infrastructure and realize ultra-broadband (gigabit speed) wireless, the application of MIMO techniques to satellite systems seems inevitable and has gained great interest due to the satellite-based modern digital video broadcasting standards DVB-SH and DVB-NGH [6]-[8]. Since channel and propagation characteristics directly determine the MIMO performance [9], a detailed knowledge and accurate characterization of the MIMO satellite radio channel for different conditions is highly critical. Efficient and reliable MIMO satellite systems can be designed, developed, and accurately tested, before their deployment. Insight on characterizing the typical narrowband Single-Input Single-Output (SISO) land mobile satellite channel at L- S-, Ku-, and Ka- frequency bands was acquired through research efforts over the last three decades [10]-[17]. The application of multi-element antennas on either the one or both sides of the radio link by forming Multiple-Input Single-Output (MISO), Single-Input Multiple-Output (SIMO), and MIMO satellite systems has only recently begun to be theoretically and experimentally investigated by academia and space agencies. The former is based on theoretical analysis and assumptions for the modeling parameters, while the latter is referred to real-world measurements and collection of measured channel data from which empirical channel models can be obtained. The communication channels can be separated by space or polarization, to offer improvements to QoS by providing diversity gain using spatial/polarization time block coding techniques, and to spectral efficiency by using spatial/polarization multiplexing or a combination of both.

The present dissertation was driven to understand the satellite-MIMO channel using circular and linear polarization in order to provide results on bit error rate (BER), system' s capacity and more importantly on the antenna's cross polarization discrimination (XPD) and the environment' s cross polarization coupling (XPC).

1.2. Dissertation Structure

The dissertation is structured and organized as follows:

Chapter 2 holds all the necessary background theory needed for wireless communications. Fundamental definitions such as wave propagation and channel fading are provided.

Chapter 3 focuses more on satellite communications presenting the satellite link at the beginning and continues with the classification of fixed and mobile satellite systems.

Chapter 4 holds a scrupulous presentation of the implementation of polarized MIMO systems. All the necessary theory is included.

Chapter 5 describes the considered system model that the present dissertation focuses on. Results derived from the link level simulation are presented and discussed in detail.

2. Wireless Communications

2.1. The wireless channel: Propagation and Fading

IN wireless communication, radio propagation refers to the behavior of radio waves when they are propagated from transmitter to receiver [18]. In the course of propagation, radio waves are mainly affected by three different modes of physical phenomena: reflection, diffraction, and scattering, all of them depicted in Figure 2-1. Reflection is the physical phenomenon that occurs when a propagating electromagnetic wave impinges upon an object with very large dimensions compared to the transmitted wavelength, for example, the surface of the earth, buildings, etc. It forces the transmit signal power to be reflected back to its origin rather than being passed all the way along the path to the receiver. Diffraction refers to the phenomenon that occurs when the radio path between the transmitter and receiver is obstructed by a surface with sharp edges or small openings. It appears as a bending of waves around the small obstacles and spreading out of waves past small openings. The secondary waves generated by diffraction are useful for establishing a path between the transmitter and receiver, even when a line-of-sight path is not present. Lastly, scattering is the physical phenomenon that forces the radiation of an electromagnetic wave to deviate from a straight path by one or more local obstacles, with small dimensions compared to the wavelength. Those obstacles that induce scattering, such as foliage are referred to as the scatterers.

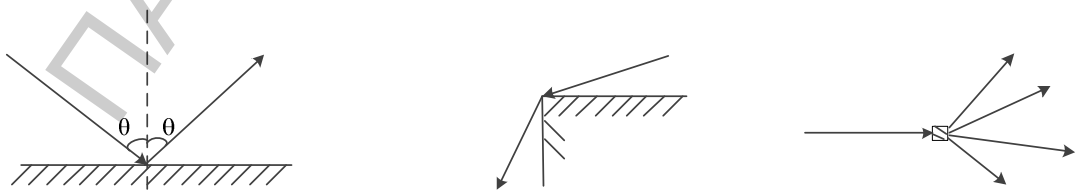

Figure 2-1: (a) Reflection, (b) Diffraction, (c) Scattering

A unique characteristic in a wireless channel is a phenomenon called *fading*, the variation of the signal amplitude over time and frequency. In contrast with the additive noise as the most common source of signal degradation, fading is another source of signal degradation that is characterized as a non-additive but multiplicative signal disturbance in the wireless channel. Fading may either be due to multipath propagation, referred to as multi-path fading, or to shadowing from obstacles that affect the propagation of a radio wave, known as shadow fading.

Path loss refers to the reduction of the power of the received signal as the distance between transmitter and receiver is increased. The reduction of the received signal power depends on the type of channel, and is usually represented by the path loss coefficient n as it is shown in (1). Depending on the type of propagation environment, the path loss coefficients can have different values (e.g. n = 2 in free space, but may go up to n = 6 in indoor environments).

$$PL = \left(\frac{4\pi d}{\lambda}\right)^n \quad or \quad PL = 10\log_{10}\left(\frac{4\pi d}{\lambda}\right)^n \ (dB) \tag{1}$$

where d is the distance from the transmitter and λ is the wavelength. Several path loss models have been developed that take into account not only the distance between transmitter and receiver, but also the type of environment, the height of transmitter and receiver etc.

If a receiver is moving at a constant distance from the transmitter, and suddenly goes behind a building, one can expect the received power to drop. This type of channel variation is called *shadowing*. In practice, shadowing is determined by considering the variations of the channel power around the path loss curve as shown in Figures 2-2 and 2-3.

The fading phenomenon can be broadly classified into two different types: large-scale fading and small-scale fading. Large-scale fading is caused by path loss of signal as a function of distance and shadowing by large objects such as buildings,

intervening terrains, and vegetation. Shadowing is a slow fading process characterized by variation of median path loss between the transmitter and receiver in fixed locations. In other words, large-scale fading is characterized by average path loss and shadowing. On the other hand, small-scale fading refers to rapid variation of signal levels due to the constructive and destructive interference of multiple signal paths (multipath). Depending on the relative extent of a multipath, frequency selectivity of a channel is characterized (e.g., by frequency-selective or frequency flat). Meanwhile, depending on the time variation in a channel due to mobile speed (characterized by the Doppler spread), short-term fading can be classified as either fast fading or slow fading. Figure 2-2 classifies all the mentioned types of fading channels.

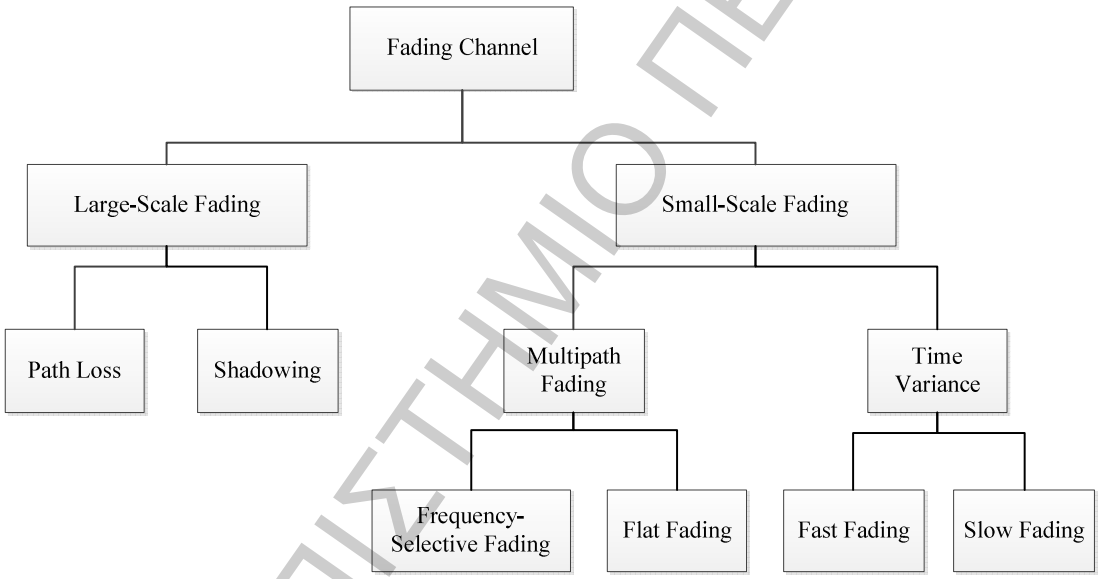

Figure 2-2: Classification of fading channels

The relationship between large-scale fading and small-scale fading is illustrated in Figure 2-3. Large-scale fading is manifested by the mean path loss that decreases with distance and shadowing that varies along the mean path loss. The received signal strength may be different even at the same distance from a transmitter, due to the shadowing caused by obstacles on the path. Furthermore, the scattering components incur small-scale fading, which finally yields a short-term variation of the signal that has already experienced shadowing.

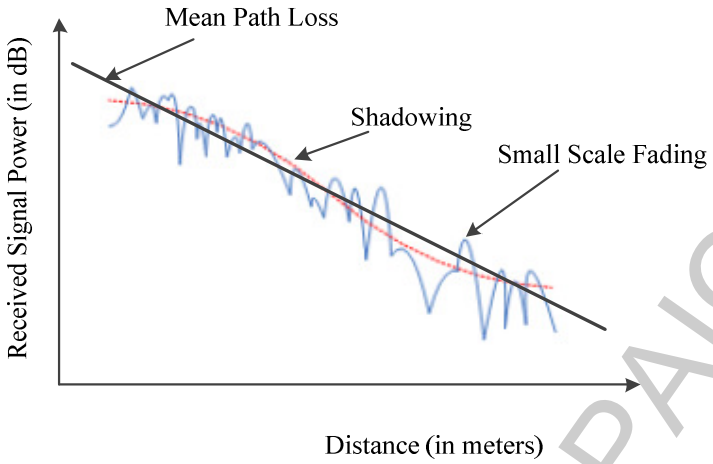

Figure 2-3: Large and Small Scale Fading

The radio channel is usually described by its baseband impulse response $h(t)$ which links the input baseband signal at the transmitter with the output baseband signal at the receiver as follows

$$y(t) = h(t) * x(t) + n(t) \tag{2}$$

where $x(t)$ and $y(t)$ are the transmitted and the received signal, respectively, and $n(t)$ represents the additive noise at the receiver. Similarly, by applying a Fourier transform on both sides of equation (2), it is possible to define the frequency dependent transfer function $H(f)$:

$$Y(f) = H(f)X(f) + N(f) \tag{3}$$

where Y , H, X and N are the Fourier transforms of y , h, x and n respectively.

2.2. Expanding to MIMO systems

In order to meet the requirements of an everyday increasing need for higher data rates and capacity the idea of implementing multiple antennas to the transmitting and receiving side of the link was adopted fast [19]. According to the number of the

antennas at each side, different configurations can be formed; the simplest configuration consists of only one antenna at each side of the link, commonly known as Single Input-Single Output (SISO). Other system configurations are the Single Input-Multiple Output (SIMO) when the transmission is done by only one antenna and the reception is completed by two or more antennas and Multiple Input-Single Output (MISO) when the signal is transmitted by multiple antennas and received by a single antenna. When combine the last two, a MIMO system occurs where multiple antennas are placed at both ends of the link. All the cases are depicted in Figure 2-4.

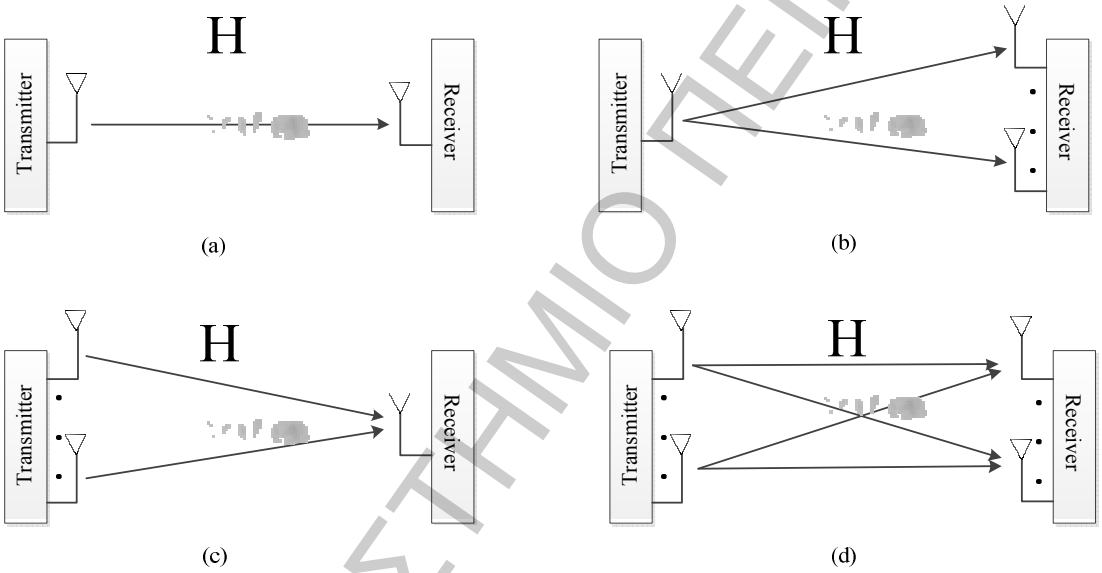

Figure 2-4: (a) SISO case, (b) SIMO case, (c) MISO case, (d) MIMO case

Let N_T and N_R be the number of transmitting and receiving antennas respectively. Then, the MIMO radio channel can no longer be described by a single element, but can be represented by the $N_R x N_T$ MIMO channel impulse response matrix $\boldsymbol{H}$ that links the input signals to the output signal [20] as follows

$$\begin{bmatrix} y_1 \\ \vdots \\ y_{N_R} \end{bmatrix} = \begin{bmatrix} h_{11} & \cdots & h_{1N_T} \\ \vdots & \ddots & \vdots \\ h_{N_R1} & \cdots & h_{N_RN_T} \end{bmatrix} \begin{bmatrix} x_1 \\ \vdots \\ x_{N_T} \end{bmatrix} + \begin{bmatrix} n_1 \\ \vdots \\ n_{N_R} \end{bmatrix} \tag{4}$$

or simpler as

$$\boldsymbol{Y} = \boldsymbol{H} \cdot \boldsymbol{X} + \boldsymbol{N} \tag{5}$$

When the channel matrix H is known to both the transmitter and the receiver, its singular value decomposition (SVD), is represented as

$$H = U \Sigma V^H \tag{6}$$

where U is an $N_R \, x \, N_R$ unitary matrix and V is an $N_T \, x \, N_T$ also unitary, so that $U^H U = I_{N_R}$ and $V^H V = I_{N_T}$ where I_{N_R} and I_{N_T} are $N_R \, x \, N_R$ and $N_T \, x \, N_T$ respectively, identities matrices, and Σ is a rectangular matrix, whose diagonal elements are non-negative real numbers and whose off-diagonal elements are zero. The diagonal elements of Σ are the singular values of the matrix $\boldsymbol{H}$, denoting them by $\sigma_1, \sigma_1, \ldots, \sigma_{\mathrm{N_{min}}}$, where $N_{\min} = \min(N_R, N_T)$.

Given the SVD of channel $\boldsymbol{H}$, the eigenvalue decomposition (EVD) can be calculated by

$$HH^H = U \Sigma \Sigma^H U^H = Q \Lambda Q^H \tag{7}$$

where $Q = U$ so that $Q^H Q = I_{N_R}$ and Λ is a diagonal matrix with its diagonal elements given as

$$\lambda_i = \begin{cases} \sigma_i^2, & i = 1, 2, \ldots, N_{\min} \\ 0, & i = N_{\min+1}, \ldots, N_R \end{cases} \tag{8}$$

The capacity of a MIMO system is given by

$$C = \log_2 \det \left[I_{N_R} + \frac{SNR}{N_T} * HH^H \right] \quad (bits / \sec / Hz) \tag{9}$$

Depending on the amount of correlation between the elements of the MIMO channel matrix, different signal processing techniques may be used. If the elements of the MIMO channel matrix are uncorrelated, diversity techniques or spatial multiplexing may be used to exploit the propagation channel [10, 11]. If the elements of the MIMO channel matrix are highly correlated, another technique, called beamforming, can be used. In this case, the multiple antennas at the transmitter and at

the receiver are used to steer the transmitted or received signals towards a certain physical direction.

Diversity techniques are usually employed to achieve a significant improvement of the system performance [18]. The principle of diversity is to provide the receiver with multiple independent versions of the same transmitted signal. If these versions are affected by independent fading conditions, the probability that all branches are in a fade at the same time reduces dramatically. When discussing diversity schemes, two gains may be introduced, array and diversity gain. These two gains insert two different improvements obtained from diversity. Figure 2-5, shows the impact of these two gains when the Error Probability is plotted against the signal to noise ratio (SNR).

Furthermore, it is important to note that when array gain occurs, it does not depend on the degree of correlation between the branches, whereas the diversity gain is maximal for independent branches and decreases as the correlation between branches increases. Another issue that is counteracted by the implementation of multiple antennas is the existence of interference. Co-channel interference arises due to frequency reuse in wireless channels. When multiple antennas are used, the differentiation between the spatial signatures of the desired signal and co-channel signals can be exploited to reduce the interference.

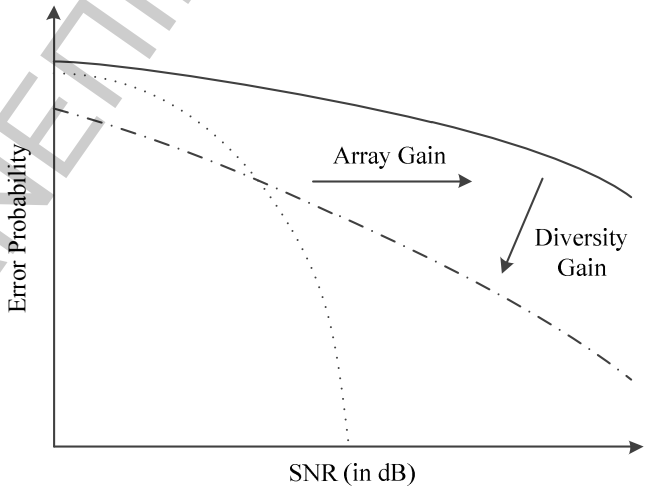

Figure 2-5: Array and Diversity Gains in a Rayleigh fading channel

2.2.1. Array gain

Array gain is the increase in received SNR that results from a coherent combining effect of the wireless signals at a receiver. The coherent combining may be realized through spatial processing at the receive antenna array and/or spatial pre-processing at the transmit antenna array. Array gain improves resistance to noise, thereby improving the coverage and the range of a wireless network.

2.2.2. Diversity gain

As mentioned earlier, the signal level at a receiver in a wireless system fluctuates or fades. Spatial diversity gain mitigates fading and is realized by providing the receiver with multiple (ideally independent) copies of the transmitted signal in space, frequency or time. With an increasing number of independent copies (also known as diversity order), the probability that at least one of the copies is not experiencing a deep fade increases, thereby improving the quality and reliability of reception.

2.2.3. Multiplexing gain

Another technique that is used to increase the transmission rate (or the capacity) of MIMO systems is spatial or polarization multiplexing. This is achieved by transmitting multiple independent data streams within the bandwidth of operation. Each data stream experiences at least the same channel quality that would be experienced by a SISO system, effectively enhancing the capacity by a multiplicative factor equal to the number of streams. In general, the number of data streams that can be reliably supported by a MIMO rich scattering channel equals the minimum of the number of transmit antennas and the number of receive antennas.

2.3. MIMO over Terrestrial

The introduction of MIMO technology now spans more than a decade with remarkable results, as it takes advantage of the rich scattering terrestrial environment [6]. The salient feature of MIMO-based systems is that all the resulting improvements come from an information theory point of view at no extra cost concerning transmit power or bandwidth.

Various MIMO techniques have been studied for terrestrial systems that have also been proposed for possible application over satellite. MIMO is a rather comprehensive term that encompasses a plethora of techniques including broad categories such as single-user (SU) and multi-user (MU).

Single-User MIMO (SU-MIMO): A point-to-point communication system that exploits multiple transmitting and receiving antennas to improve capacity, reliability, and resistance to interference.

Multi-User MIMO (MU-MIMO): A point-to-multipoint communication system where a base station (BS) with multiple transmitting and receiving antennas communicates with multiple users who may have one or more transmit and receive antennas.

MU-MIMO Advantages:

◦ In addition to stream multiplexing, MU-MIMO schemes offer MU multiplexing, resulting in a direct capacity gain proportional to the number of BS antennas and the number of users.

◦ MU-MIMO appears more immune to most of the adverse propagation phenomena resulting in a low rank SU-MIMO channel matrix, such as LoS or antenna correlation. Although increased correlation affects the diversity achieved by each user, MU diversity can be extracted instead.

◦ MU-MIMO allows for spatial multiplexing gain at the BS without necessitating terminals with multiple antennas. This is especially significant from a commercial point of view, since cost is kept in the infrastructure side.

MU-MIMO Drawbacks:

◦ Perhaps the most important disadvantage is that MU-MIMO requires Channel State Information at the Transmitter (CSIT) to perform spatial multiplexing.

◦ The MU systems users may significantly differ with respect to the channel conditions. This gives rise to fairness issues related to the selection of the subgroup of users that will be served –scheduling.

◦ In SU-MIMO, coding at the transmitter and decoding at the receiver can be done in a cooperative fashion, since the respective multiple antennas are co-located, whereas in MU-MIMO users are geographically dispersed.

3. Satellite Communications

3.1. The Satellite link

AMONG the various solutions investigated toward the enhancement of next-generation LMS systems is the upgrade from conventional SISO to advanced MIMO techniques, adopted by the terrestrial wireless community. Despite the apparent similarities of terrestrial and satellite systems, the significant differences concerning channel, system and geometrical characteristics, together with the shortage of relevant measured data render the perspectives of the MIMO approach in satellite communications uncertain.

As it was analyzed before, terrestrial propagation is affected from physical phenomena causing a rich multipath environment which creates multiple independent uncorrelated channels as it was previously shown in Figure 2-1. The satellite channel differs from a terrestrial channel due to lack of scatterers near the transmitting satellite. The result is a strong line of sight (LoS) that creates a strong channel correlation which crucially determine the performance of any potentially adopted MIMO technique. The effects of fading channel correlation mainly due to insufficient antenna spacing and sparse scattering environment at the transmitter are of primary concern as they impact the performance of MIMO communication systems. Along these lines, this section presents the most important spatial and temporal channel characteristics affecting a satellite channel.

Another important difference is the propagation environment. Ionospheric effects involve the interaction between layers of charged particles around the Earth and the radio waves. It includes ionospheric refraction, Faraday rotation [24], group delay, dispersion and ionospheric scintillation. Tropospheric effects involve the interaction between the lower layer of the Earth's atmosphere (including the air and

hydrometeors such as rain) and the radio waves. It includes attenuation, rain attenuation, gaseous absorption, tropospheric refraction, tropospheric scintillation, depolarization and sky noise.

Two large categories can be distinguished when it comes to satellite communications schemes [6], Fixed Satellite (FS) where we focus on a static link between a satellite and a Base Station (BS) and Mobile Satellite (MS) where the receiver is on the move.

3.1.1. Fixed Satellite (FS)

FS communication systems above 10 GHz operate under LoS; the satellite channel essentially corresponds to an AWGN channel. However, propagation at the Ku- and, especially, Ka- band is subjected to various atmospheric fading mechanisms originating in the troposphere, which severely degrade system performance and availability. These adverse tropospheric phenomena are briefly summarized in the following, where two categories again are appeared, long term and dynamic channel effects.

Long Term Channel Effects: The most important channel effects impairing satellite communications at frequencies above 10 GHz are summarized as follows:

- *Attenuation due to precipitation*: When propagating through snow, hail, ice droplets and, predominantly, rain, radio-waves suffer from hydrometeor scattering and absorption. This results in a flat and slow fading process proportional in dB to the square of the frequency. Hence, rain attenuation constitutes the dominant factor limiting FS system availability.
- *Gaseous absorption*: Absorption from oxygen and water vapor contributes to the total attenuation, though to a much smaller extent than rain attenuation.
- *Cloud attenuation*: The liquid water content of clouds is the physical cause of this type of attenuation.

- *Tropospheric scintillations*: This fast fading mechanism due to variations in the refractive index of the troposphere is aggravated as the frequency of operation increases.
- *Signal depolarization*: Differential phase shift and attenuation caused by non-spherical scatterers such as rain drops and ice crystals result in significant depolarization. As a result, part of the transmitted power in one polarization interferes with its orthogonal counterpart.
- *Sky Noise Increase*: As attenuation increases, so does emission noise. The same factors previously mentioned, i.e. scatter/emission from precipitation hydrometeors, contribute to noise increase.
- *Total attenuation*: The performance degradation due to the above phenomena, necessitates especially in the Ka- band. The distribution of the total attenuation over the satellite link is given by [6]:

$$A_{tot}(p) = A_g(p) + \sqrt{\left[A_c(p) + A_r(p)\right]^2 + A_s^2(p)} \tag{10}$$

where $A_g(p)$, $A_c(p)$, $A_r(p)$, and $A_s(p)$ represent gaseous, cloud, rain and scintillation attenuation for p% of annual time, respectively.

Dynamic Channel Effects: Significant research efforts have been addressed toward developing stochastic models that accurately reproduce the temporal properties of the AWGN channel when impaired by rain fading. Dynamic channel models allow for the calculation of several second order statistics, such as fade slope and fade duration. Various models have also been proposed for the generation of rain attenuation time series.

3.1.2. Mobile Satellite (MS)

Channel characteristics affecting radio-wave propagation when it comes to MS systems give rise to an entirely different channel modeling compared to the FS since two fundamental characteristics are completely different:

(i) the introduction of **user mobility** and

(ii) the use of **lower frequency bands** instead of bands above 10 GHz

Concerning the former characteristic, propagation conditions and link geometry are no longer static, insinuating that Non Line of Sight (NLoS) communication with the satellite due to heavy shadowing is a strong possibility, especially in urban environments under low elevation angles. Apart from possible degradation of the direct signal from the satellite to the Mobile Satellite Terminal (MST), the presence of nearby scatterers produces multipath propagation, which is not present in the LoS. On the other hand, transmission at the L-, S- frequency bands instead of Ku and Ka renders tropospheric phenomena irrelevant.

In general, the MS channel comprises two main signal components:

- the direct (or LoS) signal and
- the multipath (or NLoS) component due to the direct signal interacting with the scatterers in the vicinity of the MST

In turn, given these channel elements and depending on the environment the MST is operating (urban, suburban, rural, etc.) the MS channels may be classified according to:

- the degree of time dispersion (narrowband vs. wideband),
- the rate of signal variations (very slow, slow and fast variations),
- the Doppler power spectrum and
- the spatial correlation

3.2. MIMO over Satellite

The prerequisite so that single satellite configurations fully provide the spatial diversity and spatial multiplexing advantages predicted by information theory is the

existence of sufficient antenna spacing, as well as a rich scattering environment, which renders the fading paths between the antenna elements of the transmitter and the receiver independent. However, the huge distance between the satellite segments and the terrestrial stations reduces the corresponding radio link to an effective keyhole channel with only one transmission path. Then, the correlation among the MIMO sub-channels caused by a deficient multipath environment leads to a substantial loss in channel capacity from the ideal level predicted by MIMO theory. Moreover, under a multiple satellite broadcasting scenario, technical challenges arise such as lack of synchronization between the two satellites. Thus, the overwhelming majority of previous work related to multi element satellite systems has mainly focused on exploiting the following aspects of diversity and multiplexing or a combination of them:

(i) site diversity, where multiple cooperating sufficiently separated terrestrial stations communicate with a single satellite [21]-[23],

(ii) satellite (angle or orbital) diversity (Fig. 3-1a) through multiple sufficiently separated satellites and a single terrestrial station equipped with multiple single polarization antennas providing spatial multiplex channel coding [33]-[36] and

(iii) polarization techniques (Fig. 3-1b), where a single dual-polarized satellite communicates with a single terrestrial station equipped with a dual-orthogonal polarized antenna providing polarization multiplex channel coding [25]- [32].

The polarization techniques represents a promising solution due to the recent advances in MIMO compact antennas [37] and intends to overcome possible space limitations and counter possible drawbacks of multiple satellite constellations, i.e., waste of the limited satellite bandwidth for the transmission of the same signal, lack of synchronization in reception, scheduling issues, inter-symbol interference, and high implementation cost.

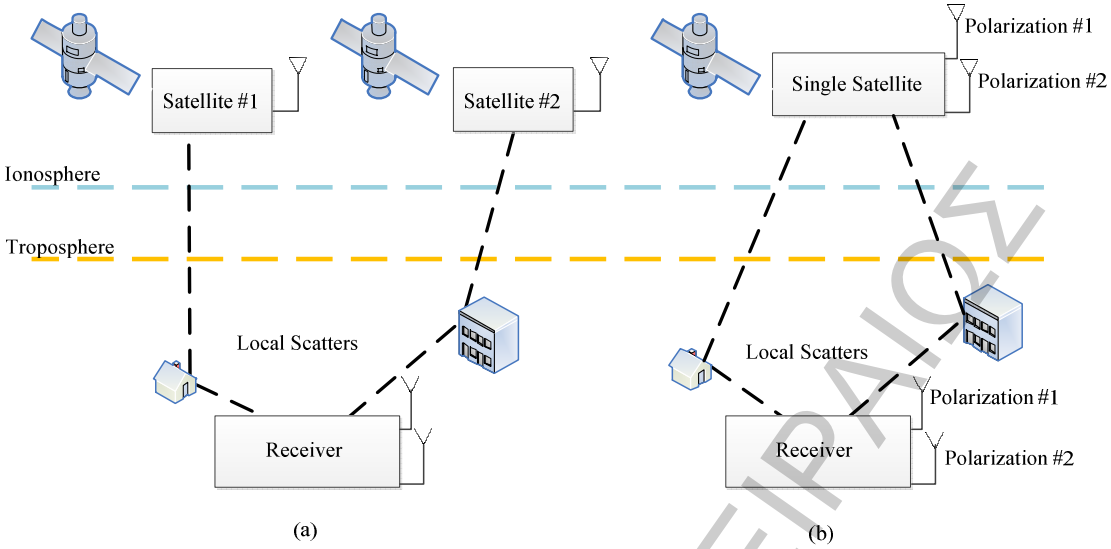

Figure 3-1: (a) Satellite and (b) Polarization Diversity

Therefore, most of previous research activities have affiliated the polarization domain. However, the polarized MIMO can only increase the throughput by a factor of two, whereas satellite diversity can result in *m*-fold capacity increase, where *m* denotes the number of satellites. Moreover, the on/off blockage phenomena and the highly correlated rainfall medium dominating at frequency bands well above 10 GHz may degrade the performance of polarized MIMO. It is worth noting that legacy terrestrial systems employ linear polarization, whereas satellite systems opt for circular polarization to overcome the effect of Faraday rotation in the ionosphere. Other ionospheric and tropospheric effects are considered negligible at L- and S-frequency bands as it was explained to the corresponding section. Therefore, the multipath propagation due to the local scattering near the terrestrial mobile stations is only of great interest for satellite MIMO systems. Note the satellite and polarized MIMO can be combined using multiple satellites each utilizing a dual-polarization scheme. Then, an extra increase in channel capacity is expected.

4. Polarized MIMO over Satellite

4.1. The need for Polarization

The appealing gains obtained by MIMO techniques in terrestrial networks generate further interest in investigating the applicability of the same principles in satellite networks. However, the fundamental differences that were analyzed in section 3.1. between the terrestrial and satellite channels make such applicability a non-trivial and non-straightforward task [38]. A possible solution to form a MIMO channel in a satellite environment is the polarization diversity. Experimental measurements have shown that when using perpendicularly polarized antennas, low inter-antenna correlation is obtained. These perpendicularly polarized antennas can be co-located, which enables the design of a compact antenna system.

A polarized MIMO system is able to exploit the polarization diversity of the channel to achieve low inter-antenna correlation: an electromagnetic wave has two orthogonal polarization components, which are independent. If the coupling between the two polarizations of the waves is low, the inter-antenna correlation between antennas capturing different polarizations will also be low. The following section is focused to a more scrupulous study regarding polarization.

4.2. Wave Polarization Theory and Analysis

The polarization of an electromagnetic wave is defined as the orientation of the electric field vector. The electric field vector is perpendicular to both the direction of travel and the magnetic field vector. The polarization is described by the geometric figure traced by the electric field vector upon a stationary plane perpendicular to the direction of propagation, as the wave travels through that plane [39].

The geometric figure traced by the sum of the electric field vectors over time is, in general, an ellipse. Under certain conditions the ellipse may collapse into a

straight line, in which case the polarization is called linear or the two components are of equal magnitude and 90° (π/2) out of phase, the ellipse will become circle. Thus linear and circular polarizations are the two special cases of elliptical polarization. Linear polarization may be further classified as being vertical and horizontal. Accordingly, circular polarization can be further categorized as right-hand circular polarization (RHCP) or left-hand circular polarization (LHCP). These four polarization configurations are shown in Figure 4-1.

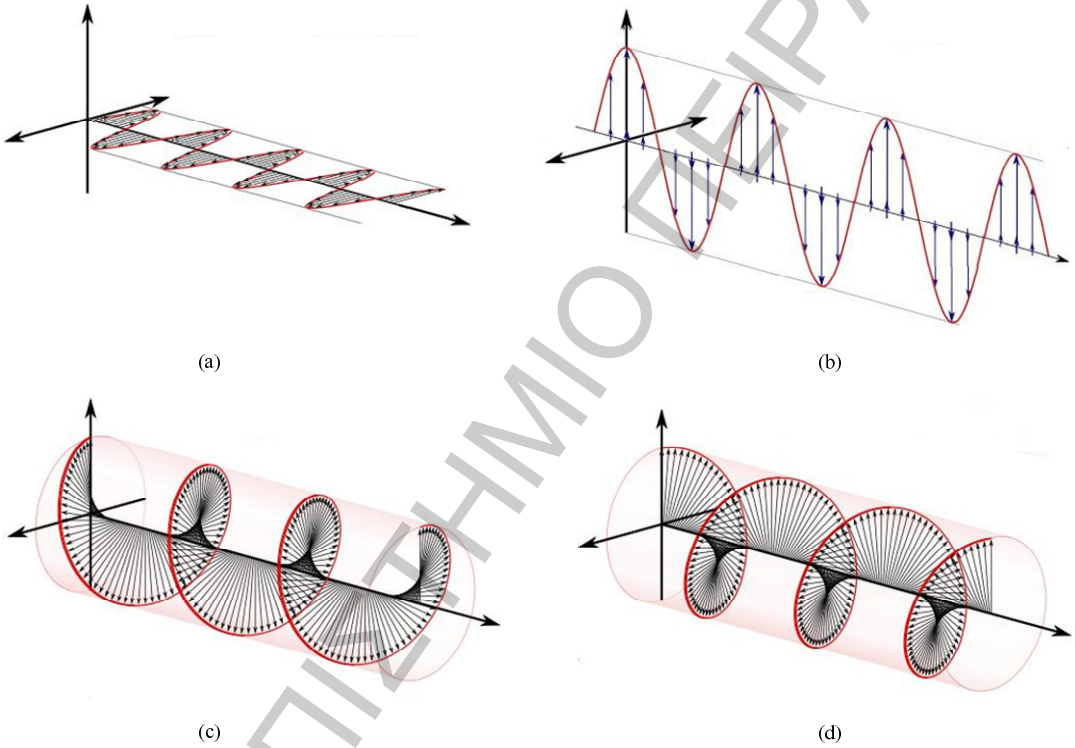

Figure 4-1: (a) Horizontal Linear Polarization, (b) Vertical Linear Polarization, (c) Right-hand Circular Polarization, (d) Left-hand Circular Polarization

It is important to mention that the sense of antenna polarization is defined from a viewer positioned behind an antenna looking in the direction of propagation. The polarization is specified as a transmitting, not receiving antenna regardless of intended use.

From a mathematical point of view, a wave when written in phasor form, can be described as

$$E_x(z) = E_1 e^{-jkz} + E_3 e^{jkz}$$
$$E_y(z) = E_2 e^{-jkz} + E_4 e^{jkz} \quad (11)$$

where E_x and E_y are the electrical fields along the x and y axis respectively, and k is the wave number. The first terms represent wave propagation in the positive z-direction, the second terms represent waves propagating in the negative z-direction. Taking only the positively traveling wave, (9) can be written in vector form as:

$$\vec{E} = \left(E_1 \hat{x} + E_2 e^{-j\psi} \hat{y}\right) e^{-jkz} \quad (12)$$

where ψ represents the phase shift between the components. For a wave propagating in any direction $\hat{r}$, the electric field solution for the wave equation in spherical coordinates is written:

$$E = \left(E_\theta \hat{\theta} + E_\varphi \hat{\varphi}\right) e^{-j\vec{k}\hat{r}} \quad (13)$$

where $\vec{k}$ is the wave vector, and E_θ, E_φ can be complex. It is clear that there are two distinct and independent components E_θ and E_φ for the wave. The relationship between E_θ and E_φ will determine the polarization of the wave.

Also, another important parameter that has to be mentioned is the *polarization ratio* of the electric fields. It is defined as:

$$\rho = \frac{E_\varphi}{E_\theta} \quad (14)$$

Observing the Figure 4-1a, in the linear case the complex fields E_θ and E_φ are in phase, and both components can have different amplitude. In the case of circular polarization the amplitude of both wave components is equal and the phase-shift between E_θ and E_φ must be π/2. In all other cases, an elliptical polarization is obtained. The ratio of the maximum to minimum polarized responses on the ellipse is the *axial ratio*. The relationship between polarization ratio and axial ratio for circularly polarized waves is [39]:

$$axial\ ratio = \begin{cases} \dfrac{E_{\max}}{E_{\min}} = \dfrac{|E_L| + |E_R|}{|E_L| - |E_R|} = \dfrac{1+|\rho|}{1-|\rho|} & LHCP \\ \dfrac{E_{\max}}{E_{\min}} = \dfrac{|E_R| + |E_L|}{|E_R| - |E_L|} = \dfrac{|\rho|+1}{|\rho|-1} & RHCP \end{cases} \quad (15)$$

where E_R and E_L are the electrical fields of right and left hand circular polarization respectively.

When considering polarized communication systems, the idea is to transmit separate data streams on each of the two polarizations of the wave. The transmitter will use two antennas to transmit two information streams on the E_θ and E_φ components of the waves, and the receiver will use two antennas that detect each of the two polarizations. Such is the case for the system model analyzed in the present dissertation; more details follow in the next chapter.

Due to the interactions of the wave with its environment, the two components of the emitted waves will be rotated in the polarization plane. In addition, scattering causes the formation of some depolarized waves i.e., from RHCP to LHCP and from LHCP to RHCP, which are represented in a 2x2 MIMO channel matrix, where there are two co-polar, RHCP to RHCP and LCHP to LHCP and two cross-polar circularly polarized channels, RHCP to LHCP and LCHP to RHCP. As a result, each antenna at the receiver will receive a mix of the two transmitted signals. Figure 4-2 shows these four channels. Note that the subscripts R and L denote the RHCP and LHCP antennas at each end of the link and n_R and n_L denote the additive white Gaussian noise (AWGN) at each receiving antenna.

Polarization rotation refers to a rotation of the polarization sense of a radio wave, caused by the interaction of a radio wave with electrons in the ionosphere, in the presence of the earth's magnetic field. This condition -referred to as the *Faraday effect*- can seriously affect very high frequency (VHF) space communications systems that use linear polarization. A rotation of the plane of polarization occurs because the two rotating components of the wave progress through the ionosphere with different

velocities of propagation. This is the reason why when it comes to satellite communication, circular polarization is preferred.

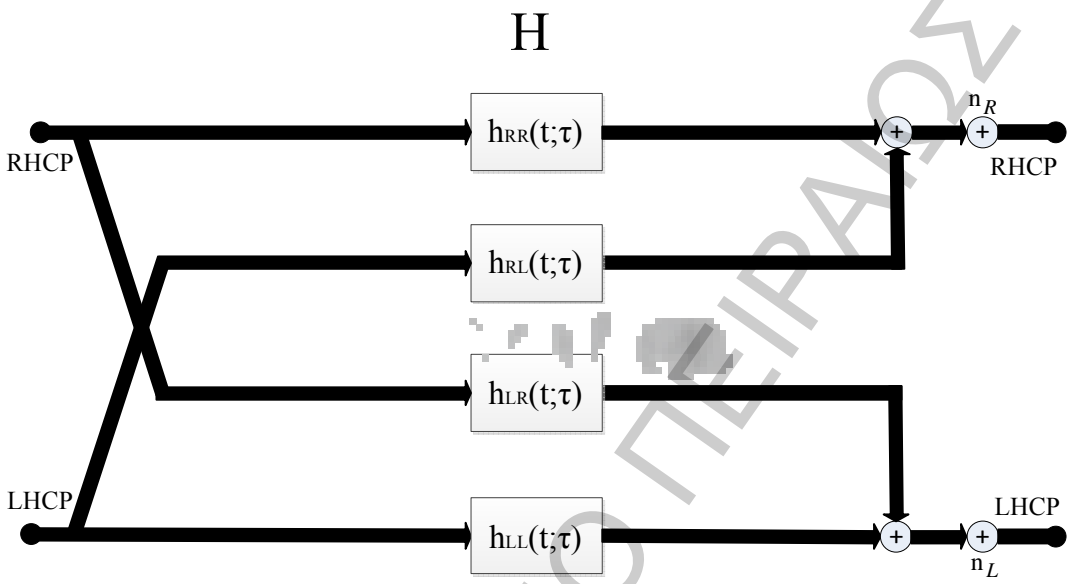

Figure 4-2: Polarization Channels

4.2.1. Antenna Polarization

Any electric conductor that transports a time-varying electrical current will transmit electromagnetic radiation. If the conductor is designed to transmit or receive such electromagnetic waves, it is called an *antenna* [39]. Antennas are defined by several fundamental parameters. In the context of polarization analysis, it is especially the antenna's radiation pattern that is of importance. The radiation pattern of an antenna describes the electromagnetic far fields that are transmitted when an antenna is excited by a current. Since an antenna is a passive electrical device, by reciprocity, the radiation pattern can also be used to define the receiving properties of the antenna. In that case, the radiation pattern describes the response at the output of the antenna when being illuminated by an electromagnetic wave.

Three regions around the antenna are defined: the near-field, the Fresnel region and the far-field (Fraunhofer) region. In the near field and the Fresnel zone the angular radiation pattern is dependent on the distance from the antenna. In the far-field, the radiation pattern will depend only on the angular direction and not on the distance from the antenna, and transmitted waves will be approximately planar. In this case, the radiation pattern of the antenna is

$$\vec{f}(\theta,\varphi) = f_\theta(\theta,\varphi)\hat{\theta} + f_\varphi(\theta,\varphi)\hat{\varphi} \tag{16}$$

An antenna can be designed to mainly transmit or receive one polarization. However, the polarization of the waves that will be transmitted or received can also be dependent of the direction of transmission or arrival of the waves. Real-world antennas will always have the two components for the radiation patterns. Even if an antenna is mainly designed to transmit one polarization, its imperfect nature will cause it to also transmit on the perpendicular polarization, so it will radiate an electromagnetic wave that will have both polarizations. Polarization mismatch adds an extra loss. If a signal $x(t)$ is sent at the input of the antenna, the free-space radiated far-field will be (where the vector notation has been replaced by a matrix notation)

$$\begin{bmatrix} E_\theta(\theta,\varphi,t) \\ E_\varphi(\theta,\varphi,t) \end{bmatrix} = \frac{e^{-j\vec{k}\vec{r}}}{r} \begin{bmatrix} f_\theta(\theta,\varphi) \\ f_\varphi(\theta,\varphi) \end{bmatrix} x(t) \tag{17}$$

where r is the distance from the antenna. In this notation, all antenna effects are included in the $\boldsymbol{f}$ vector (antenna mismatch, antenna efficiency, etc.). In the case of a vertical linear antenna, the f_θ component will be large and the f_φ component will be small, resulting in a wave with a large E_θ component and a small E_φ component.

On the other hand, when a wave $\vec{\mathrm{E}} = \begin{bmatrix} E_\theta & E_\varphi \end{bmatrix}^{\mathrm{T}}$ arrives on an antenna with incidence angles (θ,φ), the signal $y(t)$ at the output of the antenna is given by:

$$y(t) = \begin{bmatrix} f_\theta(\theta,\varphi) & f_\varphi(\theta,\varphi) \end{bmatrix} \begin{bmatrix} E_\theta(t) \\ E_\varphi(t) \end{bmatrix} = E_\theta f_\theta(\theta,\varphi) + E_\varphi f_\varphi(\theta,\varphi) \tag{18}$$

Recalling Figure 4-2, it is understood that the signal at the output of the receiver is composed of four terms:

- the first term is the signal component that is transmitted on the θ polarization of the wave, remained unaltered by scattering and received on the θ polarization of the receive antenna.
- the second term is the signal component that is transmitted on the φ polarization of the wave, part of it was transformed in the θ polarization due to scattering and received on the θ polarization of the receive antenna.
- the third term is the signal component that is transmitted on the θ polarization of the wave, part of it was transformed in the φ polarization due to scattering and received on the φ polarization of the receive antenna.
- the final term is the signal component that is transmitted on the φ polarization of the wave, remained unaltered by scattering and received on the φ polarization of the receive antenna.

4.2.2. Cross Polarization Discrimination

In general, a flat surface or sphere will reflect a linearly polarized wave, for example, with the same polarization as received. A horizontally polarized wave may get extended range because of water and land surface reflections, but signal cancellation will probably result in "holes" in coverage. Reflections will reverse the sense of circular polarization.

Depolarization refers to a change in the polarization characteristics of the radio wave as it propagates through the atmosphere. Depolarization can occur for linear and for circular polarized systems [40]. A depolarized radio wave will have its polarization state altered such that power is transferred from the desired polarization state to an undesired orthogonally polarized state, resulting in interference or crosstalk between the two orthogonally polarized channels.

The major causes of depolarization are rain in the path, high altitude ice particles in the path, and multipath propagation. Cross polar discrimination (XPD) is a measure of how much of a signal in a given polarization is scattered into the opposite polarization by the medium alone and is defined for the LHCP waves as

$$XPD_{LHCP} = 20\log\left(\frac{|E_{LL}|}{|E_{RL}|}\right) \ (dB) \tag{19}$$

and for the RHCP, as

$$XPD_{RHCP} = 20\log\left(\frac{|E_{RR}|}{|E_{LR}|}\right) \ (dB) \tag{20}$$

where E_{LL} and E_{RR} are the received electric field in the co-polarized (desired) and E_{LR} and E_{RL} are the electric fields converted to the orthogonal cross-polarized (undesired). Corresponding equations are used in case of linear polarization between the vertical and the horizontal received electric fields.

An alternative method to calculate the XPD for dual circular polarization is through the axial ratio mentioned in section 4.2.:

$$XPD = 20\log\left(\frac{ar+1}{ar-1}\right) \ (dB) \tag{21}$$

where ar is the axial ratio as defined in equation (13).

A closely related parameter is the isolation [39], [40], XPI, which compares the co-polarized received power with the cross-polarized power received in the same polarization state or in other words the isolation parameter shows how much two signals of opposite polarizations transmitted simultaneously will interfere with each other at the receiver.

$$XPI_{LHCP} = 20\log\left(\frac{|E_{LL}|}{|E_{LR}|}\right) \ (dB) \tag{22}$$

for the LHCP, and

$$XPI_{RHCP} = 20\log\left(\frac{|E_{RR}|}{|E_{RL}|}\right) \ (dB) \tag{23}$$

for the RHCP case.

Isolation takes into account the performance of the receiver antenna, feed, and other components, as well as the propagating medium. When the receiver system polarization performance is close to ideal, the XPD and XPI are nearly identical, and only the propagating medium contributes depolarizing effects to system performance.

All in all, Figure 4-3 shows a list of propagation mechanism and their effect to specific system parameters.

4.3. Measurement Campaigns

Countless measurement campaigns have been conducted in an attempt to shed light on a variety of recent research activities with reference to the characterization of the broadband satellite radio channel through measurements, when multi-antennas are used. Since the experiments are performed in specific areas, where the influence of the fluctuating direct and diffuse components of the signal significantly differs, an adequate number of real-time field trials in different environments, i.e., dense-urban, urban, sub-urban, highway, tree-line road, rural, open, and indoor areas, is required to accurately determine the benefits of MIMO satellite systems. Numerous critical system parameters should be included, such as the choice of orbit, the user mobility (fixed vs. mobile systems), the operating frequency band, the group size of intended users (broadcast, multicast, unicast), the multiplexing scheme, and the type of application. The variation of the elevation angle of the satellite due to its orbital motion was also studied and quantified, since this variation has an influence on shadowing and multipath reception.

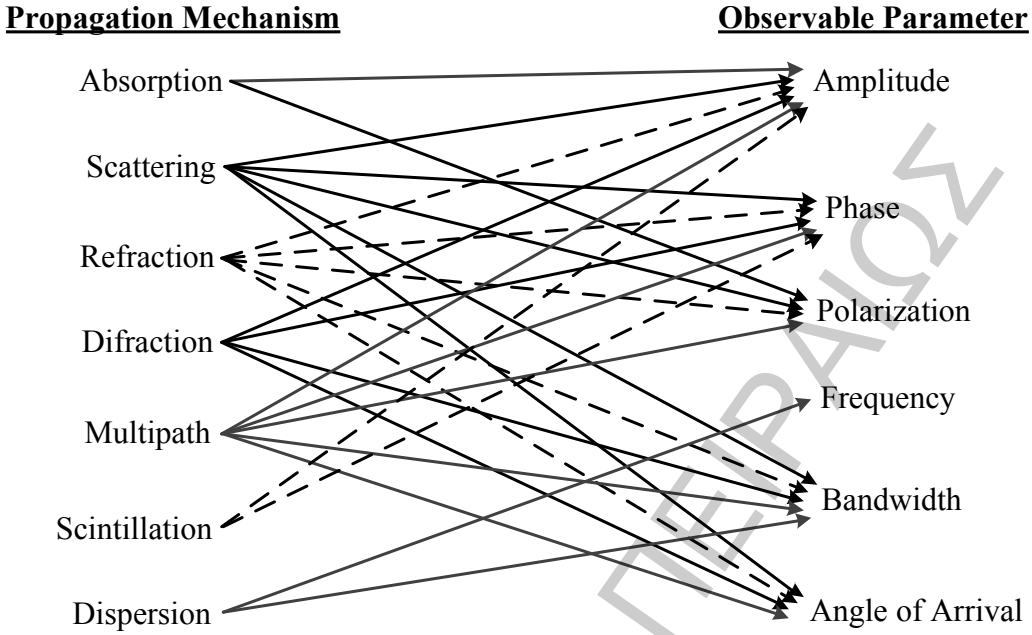

Figure 4-3: Propagation mechanisms and affected parameters

Two very important contributions are going to be presented next showing the significance of implementing polarization to MIMO systems. Both these papers come from the University of Surrey and are authored by Peter R. King and Stavros Stavrou [25], [35].

1. Capacity Improvement for a Land Mobile Single Satellite MIMO System

The paper is based on measurements using a dual circularly polarized 2x2 MIMO system comprised a terrestrially based artificial platform to represent a low elevation single satellite [25]. The transmitter consisted of two antennas one directional RHCP and one directional LHCP antenna, spaced just under one wavelength apart. The artificial platform was situated on a hilltop, communicating at S-band frequencies, with a mobile vehicle (van). Three environments were tested, tree-lined road, suburban and urban. The satellite elevation angles ranged from 7˚ - 18˚, 5˚ - 10˚ and 5˚ - 15˚, for the three environments respectively. It is important to mention that in order to reduce scattering local to the artificial platform, antennas were mounted 6 meters above ground.

From the receiver's point of view, the van was fitted with omnidirectional RHCP and LHCP antennas spaced four wavelengths apart. Vehicle speeds were 8.9m/s in the tree-lined road environment, and 5.6m/s in the suburban and urban environments, representing a typical daytime traffic flow speeds in each environment.

For the measurements an Elektrobit Propsound wideband MIMO channel sounder was configured for a carrier frequency of 2.45 GHz transmitting a direct-sequence spread spectrum signal, produced from binary-phase-shift-keyed modulated pseudo-noise codes.

After normalizing each channel matrix at each position relative to the FSL and adding a realistic fade margin, the directional antenna gain at each elevation angle was recorded and the normalized MIMO channel matrix was obtained. Then, the available channel capacity was estimated for main road, suburban and urban environments and for 15 dB receive single-to-noise ratio (SNR). The results regarding the received power relative to FSL distributions for co-polarized and cross-polarized components depicted that the co-polarized channel components are greater than the cross-polarized component for the main road and the suburban area and higher received power levels. However, this difference is minimized for the urban area and is nullified at lower received powers. Moreover, the capacity results revealed that a dual-polarized 2x2 satellite MIMO system significantly overcomes the performance of a single-polarized satellite SISO system. A comparison between capacity results from a SISO, and a Dual Polarized Single Satellite (DP-SS), dual polarized antenna terminal (2x2 MIMO) system has been made in order to show the benefits of polarized MIMO over satellite.

2. Characteristics of the land mobile satellite MIMO channel

The second paper presents again a low elevation scenario implementing an artificial platform with two emulated, adjacent positioned satellites each with a right hand circular polarized antenna [35]. They were communicating with a vehicle containing two co-polarized antennas. Each emulated satellite was separated by 10

wavelengths corresponding to two geostationary satellites. To the other end, each patch antenna on the vehicle was separated by 4 wavelengths.

An Elektrobit Propsound wideband MIMO channel sounder was used with the same configuration. The results obtained from the survey refer to outage capacity showing the benefit of utilizing dual satellites in a land mobile satellite MIMO scenario.

Table I -followed by graphical representations- gathers the numerical results for the outage capacity from those two measurement campaigns. All the tested environments are included for both SISO and MIMO cases.

Table I: Values for outage Capacity results for all tested environments for SISO and MIMO cases

SNR=15dB	Outage Capacity (bits/sec/Hz)							
	Single Satellite-Dual Polarization				Dual Satellite-Single Polarization			
	SISO		MIMO		SISO		MIMO	
	10%	50%	10%	50%	10%	50%	10%	50%
Road	0,02	0,39	0,14	0,96	0,06	0,62	0,12	1,13
Suburban	0,09	0,8	0,37	1,35	0,06	0,44	0,12	0,84
Urban	0,03	0,27	0,26	0,67	0,12	0,33	0,24	0,63

Comparing the values between the SISO and MIMO case from Table I we can conclude that for the MIMO case the outage capacity almost tripled.

Observing Figures 4-4 and 4-5 the Single Satellite-Dual Polarization (SS-DP) system performs better than the Dual Satellite-Single Polarization (DS-SP) for the MIMO case, suggesting that using dual polarization is more beneficial than implementing two transmitters. An interesting result raised from the measurements is that capacity is smaller in urban areas probably due to the increased strength of the LoS component and the spatial correlation introduced.

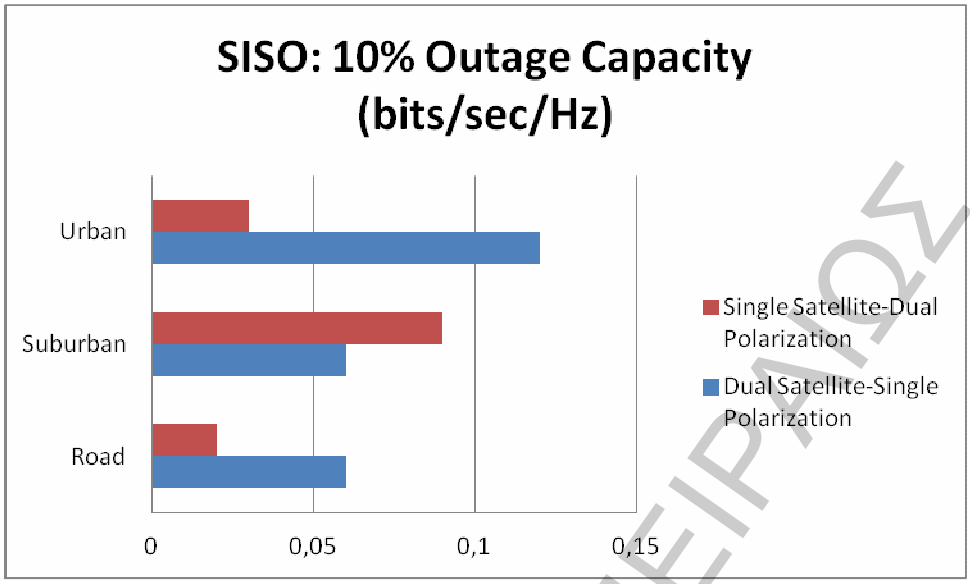

Figure 4-4: 10% SISO Outage Capacity for 15 dB SNR for all tested environments

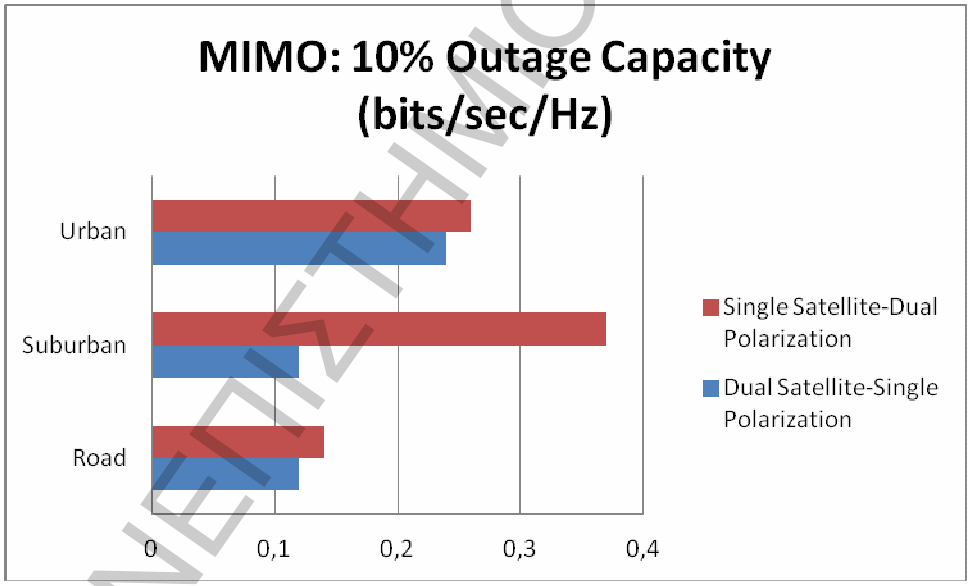

Figure 4-5: 10% MIMO Outage Capacity for 15 dB SNR for all tested environments

4.3.1. Conclusions

It is envisaged that multi-antenna satellite systems will be potentially capable of providing and delivering a compelling range of current and next generation mobile and fixed services. By validating the advantages of applying MIMO technology to satellite networks, the satellite operators and system designers will design and construct new types of satellite broadcasting systems. Although the results from current real-world channel-sounding measurement campaigns constitute a robust basis for the characterization of the multi-antenna satellite channel and are indicative of a promising evolution for MIMO satellite communications, the experiments were performed in specific areas, where the influence of the fluctuating direct and diffuse components of the signal significantly differs. Therefore, future research efforts may be devoted to collecting measured channel data in different areas, improve and/or extend the validity of current results, and accurately determine the benefits of MIMO technology over satellite systems. Moreover, experimentally characterizing MIMO LMS systems operating at mm-wave frequencies are necessary, in order to investigate the performance of future broadband applications, such as the provision of high-speed Internet access, audio and video on demand and file transfer to vehicles, airplanes, trains and ships [41]. Then, both local environment propagation effects, e.g., multipath, shadowing, and blockage due to the local environment in the vicinity of the terrestrial receiver, and tropospheric effects, e.g., rainfall, oxygen absorption, water vapor, clouds, and precipitation, are involved.

5. Polarized 2x2 MIMO System Simulation

5.1. System Model

ALTHOUGH, there are no available channel models to simulate a MIMO LMS scenario, statistical channel models have been carefully designed step by step using specific parameters of interest derived from countless measurement campaigns. Figure 5-1 illustrates the 2x2 MIMO LMS channel scenario under consideration. A single satellite employs a dual polarization scheme with two cases: (a) dual linear polarization (vertical and horizontal), (b) dual circular polarization (right- and left-handed). More specifically, the transmitter consists of a single antenna capable of dual-polarization outputs, with the multiple antenna elements to be co-located on each side of the transmission link assuming no spatial separation between them. To the other end, the User Terminal (UT) employs the similar polarization scheme used by the transmitter.

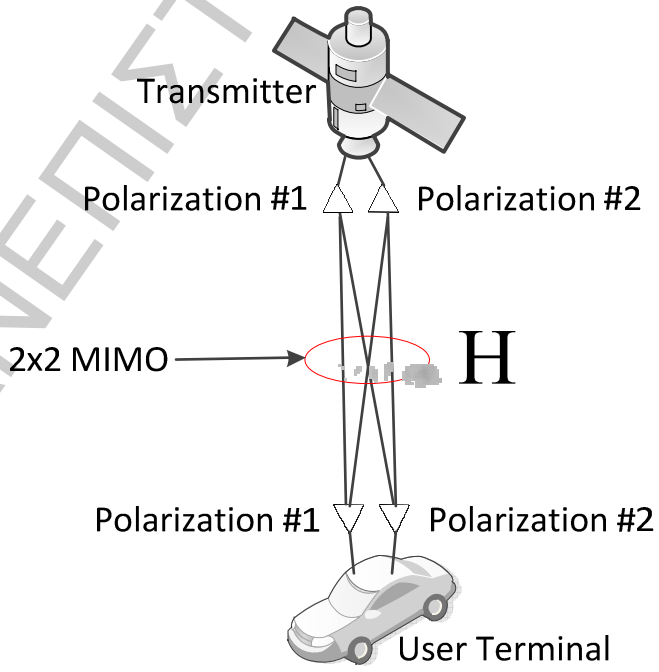

Figure 5-1: The 2x2 MIMO LMS channels (dual polarization diversity configuration)

Due to the local environment in the vicinity of the UT, the LOS link might be clear, partially or fully obstructed by trees or buildings for example, which gives rise to multipath, shadowing and blockage effects, respectively. The resulting fading channel is assumed narrowband since the multipath echoes are not significantly spread in time. Under the assumptions above, the MIMO LMS channel can be modeled by a 2x2 MIMO channel matrix $H = [h_{ij}]\ (i, j = 1, 2)$, where h_{ij} represents the fading components of the SISO LMS sub-channels formed between the transmit and receive sides as they are shown in Figure 5-1, which incorporate both the large-scale fading effects (direct LOS shadowing) and the small-scale fading effects (diffuse multipath) [16].

5.1.1. SISO LMS Sub-Channels

For the modeling of the envelope h_{ij} $(i, j = 1, 2)$, the Loo (or shadowed-Ricean) distribution [46], [47] is assumed because it has been fundamental to the building of the SISO LMS channel model, which has been extensively used and validated in the recent standardization activity of DVB-SH. Under this assumption, the 2x2 MIMO LMS channel matrix H is expanded as

$$H = [h_{ij}] = [\overline{h}_{ij}] + [\tilde{h}_{ij}] = \overline{H} + \tilde{H} \quad (i, j = 1, 2) \tag{24}$$

and

$$h_{ij} = \left|h_{ij}\right| \exp\left(j\varphi_{i,j}\right) = \left|\overline{h}_{ij}\right| \exp\left(j\overline{\varphi}_{i,j}\right) + \left|\tilde{h}_{ij}\right| \exp\left(j\tilde{\varphi}_{i,j}\right) \quad (i, j = 1, 2) \tag{25}$$

and

$$p\left(\left|h_{ij}\right|\right) = \frac{\left|h_{ij}\right|}{b_0\sqrt{2\pi d_0}} \times \int_0^\infty \frac{1}{z} \exp\left[-\frac{\left(\ln z - \mu\right)^2}{2d_0} - \frac{\left|h_{ij}\right|^2 + z^2}{2b_0}\right] I_0\left(\frac{\left|h_{ij}\right| z}{b_0}\right) dz \tag{26}$$

where $p(.)$ is the Loo probability density function, $a = 20\log_{10}(\exp(\mu))$ and $\psi = 20\log_{10}(\exp(\sqrt{d_0}))$ are the mean and standard deviation, respectively, of the log-

normally distributed envelope $\left|\overline{h}_{ij}\right|$ of the large-scale fading components, $MP = 10\log_{10}(2b_0)$ is the average power of the Rayleigh distributed envelope $\left|\tilde{h}_{ij}\right|$ of the small-scale fading components, and $I_0(\Delta)$ is the modified Bessel function of first kind and zero order. The Loo statistical parameter triplet (α, ψ, MP) refers to the experimental dataset which is originally presented in [45]. Depending on the frequency, the environment and the angle of elevation used in each case a different parameter triplet is chosen. The available choices for the frequencies are L (1/2 GHz) and S (2/4 GHz) bands, for the environment option; intermediate/heavy/light tree shadowed, urban, suburban, open rural; and for the elevation angles: $\theta = 40^{\circ} - 80^{\circ}$ (S-band) and $\theta = 10^{\circ} - 70^{\circ}$ (L-band). The methodology to obtain the Loo statistical parameters (α, ψ, MP) based on tabulated experimental datasets is detailed in [45].

5.1.2. Environment XPC and Antenna XPD

The large-scale fading components $\bar{h}_{ij}$ $(i, j = 1, 2)$ are related only to the cross-polar discrimination of the antenna, denoted by XPD_{ant}, whereas the small-scale fading components $\tilde{h}_{ij}$ $(i, j = 1, 2)$ are related to both XPD_{ant} and the XPC_{env} which denotes the cross polarization coupling of the environment. The XPD_{ant}, is calculated after the signal has been received by the UT whereas the XPC_{env} , is calculated right before the signal's reception, as it depends only on the propagation channel. The XPD_{ant} in most practical configurations of satellite networks is not greater than 15dB. On the contrary, the XPD of the satellite antenna is assumed to approximate ∞ due to its practically very large value. Thus, the variable XPD_{ant} will denote hereinafter only the UT antenna XPD.

The Branch Power Ratio revels the power imbalance between the co- and cross- polar components in the cases of 0°/90° and ±45° polarization diversity configurations and is defined (in dB) as

$$BPR = 10\log_{10}\left(\frac{E\left[\left|h_{11}\right|^2\right]}{E\left[\left|h_{22}\right|^2\right]}\right) \tag{27}$$

where $E[.]$ denotes the expectation operator. The power of the small- and large-scale fading components is given by

$$E\left[\left|\bar{h}_{ij}\right|^2\right] = \begin{cases} \left(\psi^2 + \alpha^2\right) * \left(1 - \beta_{ant}\right) & i = j \\ \left(\psi^2 + \alpha^2\right) * \beta_{ant} & i \neq j \end{cases} \tag{28}$$

$$E\left[\left|\tilde{h}_{ij}\right|^2\right] = \begin{cases} MP * \left(1 - \gamma\right) & i = j \\ MP * \gamma & i \neq j \end{cases} \tag{29}$$

where $i, j = 1,2$, (α, ψ,MP) are expressed in linear scale (not in dB), $\beta_{ant} \in [0,1]$

depends only on XPD_{ant} and $\gamma \in [0,1]$ depends on both XPD_{ant} and XPC_{env}. Concerning the relationship between the XPD modeling factors β_{ant} and γ in [19], [42] as well as the actual measurable parameters XPD_{ant} and XPC_{env} are

$$XPD_{ant} = 10\log_{10}\left(\frac{E\left[\left|\bar{h}_{ii}\right|^2\right]}{E\left[\left|\bar{h}_{ji}\right|^2\right]}\right) = 10\log_{10}\left[\frac{(1-\beta_{ant})}{\beta_{ant}}\right] \tag{30}$$

$$XPC_{env} = 10\log_{10}\left[\frac{(1-\gamma_{env})}{\gamma_{env}}\right] \tag{31}$$

where

$$\gamma = \beta_{ant}(1-\gamma_{env}) + (1-\beta_{ant})\gamma_{env} \tag{32}$$

Alternatively both XPD and XPC can be calculated using the axial ration as in equation (19).

5.2. Linear detection Methods

If the transmitter does know the channel, there is an architecture called Singular Value Decomposition (SVD) that enables the transmitter to send parallel data streams along the eigenmodes of the channel. So the streams arrive orthogonally at the receiver without interference between each other. In case the transmitter does not know the channel, this is not possible. Indeed, after passing through the MIMO channel, the independent data streams all arrive cross-coupled at the receiver. It is of great importance that the receiver can separate the data streams efficiently [43].

Linear signal detection method treats all transmitted signals as interferences except for the desired stream from the target transmit antenna. Therefore, interference signals from other transmit antennas are minimized or nullified in the course of detecting the desired signal from the target transmit antenna. To facilitate the detection of desired signals from each antenna, the effect of the channel is inverted by a weight matrix W such that:

$$\tilde{x} = \left[\tilde{x}_1 \tilde{x}_2 \ldots \tilde{x}_{N_T} \right]^T = Wy \tag{33}$$

that is, detection of each symbol is given by a linear combination of the received signals. The standard linear detection methods include the zero-forcing (ZF) technique and the minimum mean square error (MMSE) technique.

5.2.1. Zero Forcing Receivers

The zero-forcing (ZF) technique nullifies the interference at the receiver by the following weight matrix

$$W_{ZF} = \left(H^H H \right)^{-1} H^H \tag{34}$$

where $(.)^H$ denotes the Hermitian transpose operation. In other words, it inverts the effect of channel as

$$\tilde{x}_{ZF} = W_{ZF} y = x + \left(H^H H \right)^{-1} H^H n = x + \tilde{n}_{ZF} \tag{35}$$

where $\tilde{n}_{ZF} = \left(H^H H \right)^{-1} H^H n$. As it is shown in Figure 5-2, each stream $y_1, y_2, \ldots, y_{N_T}$ is multiplied with the corresponding weight $W_1, W_2, \ldots, W_{N_T}$ resulting to the estimated stream $y'_1, y'_2, \ldots, y'_{N_T}$.

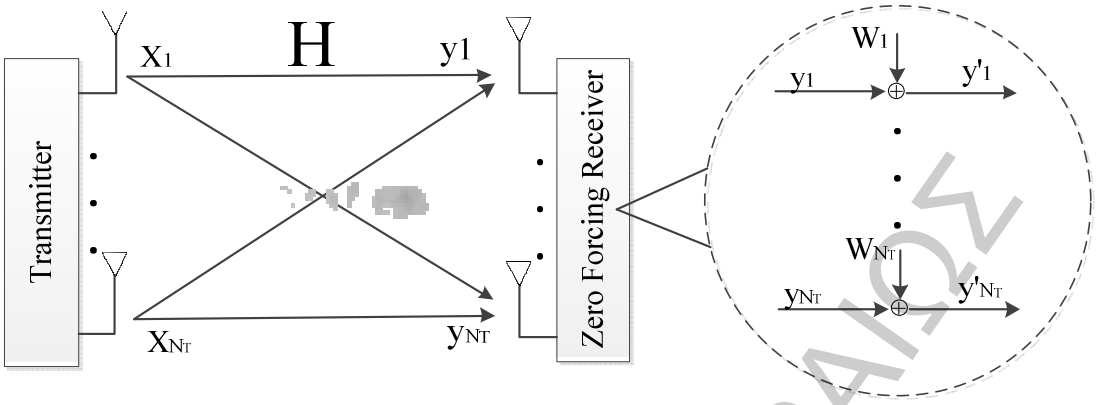

Figure 5-2: A Zero Forcing Receiver (and after ZF nulling operation)

5.2.2. Minimum Mean Square Error Receivers

In order to maximize the post-detection Signal to Interference plus Noise Ratio (SINR), the MMSE weight matrix is given as

$$W_{MMSE} = \left(H^H H + \sigma_n^2 I_{N_T} \right)^{-1} H^H \tag{36}$$

Note that the MMSE receiver requires the statistical information of noise σ_n^2. Using the MMSE weight in equation 34, we obtain the following relationship:

$$\tilde{x}_{MMSE} = W_{MMSE} y = x + \left(H^H H + \sigma_n^2 I \right)^{-1} H^H n = x + \tilde{n}_{MMSE} \tag{37}$$

where $\tilde{n}_{MMSE} = \left(H^H H + \sigma_n^2 I \right)^{-1} H^H n$.

5.2.3. Successive Interference Cancellation

Once a data stream is successfully recovered using the methods that were described earlier, it can be subtracted from the received vector and reduce in this way the burden on the receiver of the remaining data streams. This technique is known as Successive Interference Cancellation (SIC). Assuming the first stream x_1 is successfully decoded, the second Zero-Forcing detector only needs to deal with

streams $x_3,\ldots,x_{N_T}$ as interference, since x_1 has been correctly subtracted off. Thus, the second Zero-Forcing detector projects onto a subspace which is orthogonal to $h_3,\ldots,h_{N_T}$. This process is continued until the last Zero-Forcing detector does not have to deal with any interference from the other data streams. It is assumed subtraction is successful in all preceding stages.

However, a significant problem is observed with this receiver structure. It is called error propagation; if an error occurs in detecting the $k\,th$ data stream, it will make the subtracted signal incorrect. Furthermore, this error will propagate to all the following streams, $k+1,\ldots,N_T$. If it is assumed that the data streams are well coded and the block length is sufficient large, then the probability of the streams being successfully cancelled is very high. With this assumption, the $k\,th$ data stream experiences no up-stream interference, i.e., from the streams $1,\ldots,k-1$.

When SNR is high, the inter-stream interference is dominant over the additive Gaussian noise, Zero-Forcing detector performs well but when SNR is low, the inter-stream interference is not as much of an issue, matched filter is the best choice. Given this situation, a linear receiver is needed which optimally trades off between the inter-stream interference and the background Gaussian noise. A MMSE receiver seems like a solution to accomplish the desired goal. It replaces Zero-Forcing detectors with Minimum Mean-Square Error detectors. This MMSE receiver scheme performs as a Zero-Forcing detector when inter-stream interference is high, and as a matched filter when interference is low. Figure 5-3 depicts the SIC process using ZF or MMSE detectors for stream estimation.

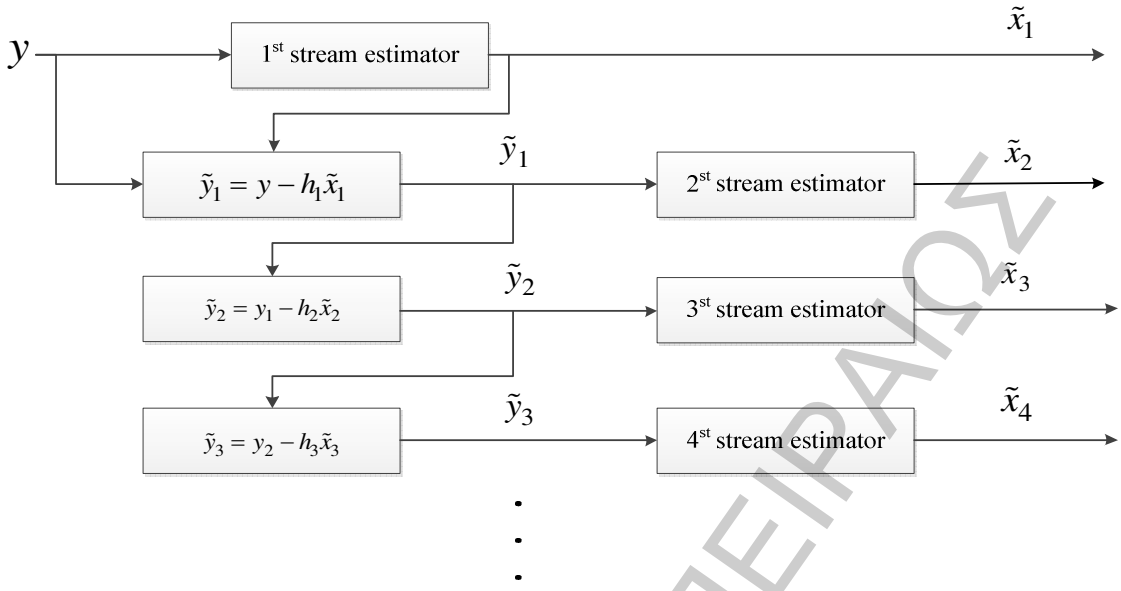

Figure 5-3: Illustration of SIC method

5.3. MATLAB Simulation

The general idea behind building the MATLAB code to simulate the analyzed system model is shown graphically in Figure 5-4. A random bit stream for each antenna is generated and then phase shifted accordingly to the type of polarization chosen to be used, for example, circular and right handed. Continuing, the transmitted signals are affected from the propagation channel H which as mentioned in section 5.1, is modeled using the Loo distribution. At the receiver side, using the methods described in section 5.2 the bit streams are retrieved, followed by the depolarization process of each received stream where a phase shift takes place again but to the opposite direction used to polarize the streams. Then the calculation of Bit Error Rate (BER), XPD (XPD_{ant} and XPC_{env}) and finally, system's capacity is possible given the aforementioned equations in section 5.1.

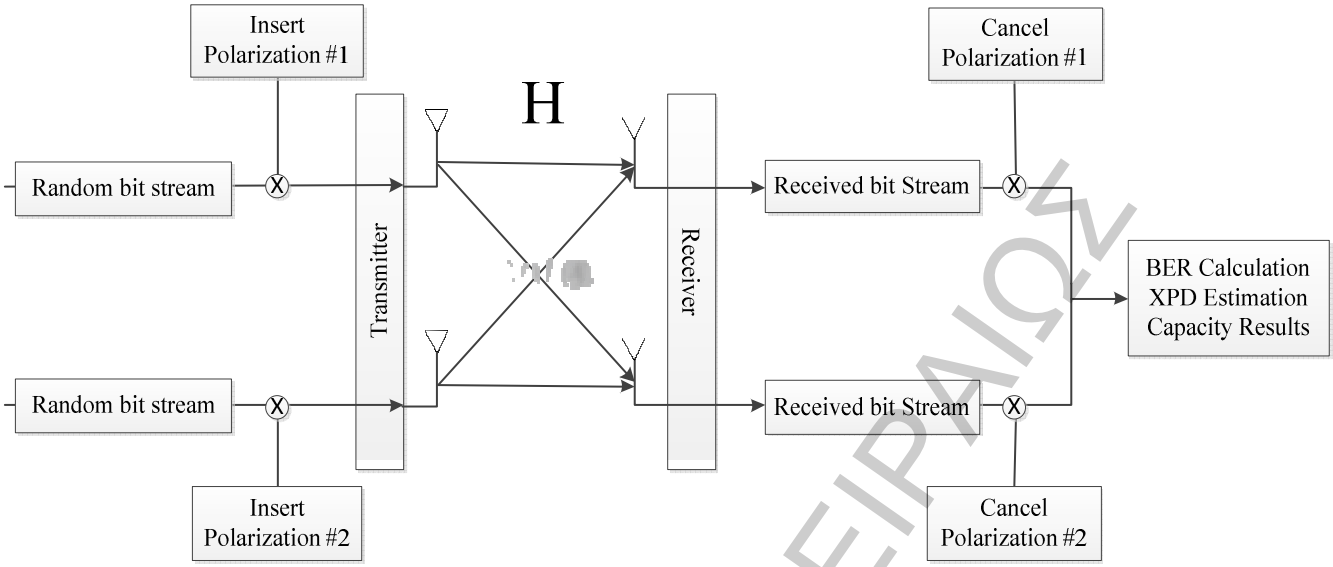

Figure 5-4: Graphical representation of MATLAB simulation code

5.4. From Theory to Implementation

Using MATLAB several scripts were built to evaluate the performance of the mentioned parameters each time using different scenarios implementing for example, ZF, MMSE, SIC ZF or SIC MMSE receivers into different environments such as heavy/light shadowed urban, suburban, rural, tree line road etc. In all cases, 4-QAM modulation is chosen to be implemented.

To begin with, the results for the BER are presented classified by the type of polarization used (circular and linear). Note that the blue line represents the simulated case when using ZF detection whereas the cyan line represents an MMSE receiver. The green and pink lines which show the theoretical SISO and the AWGN SISO correspondingly, are used as reference in order to have a better understanding of the results.

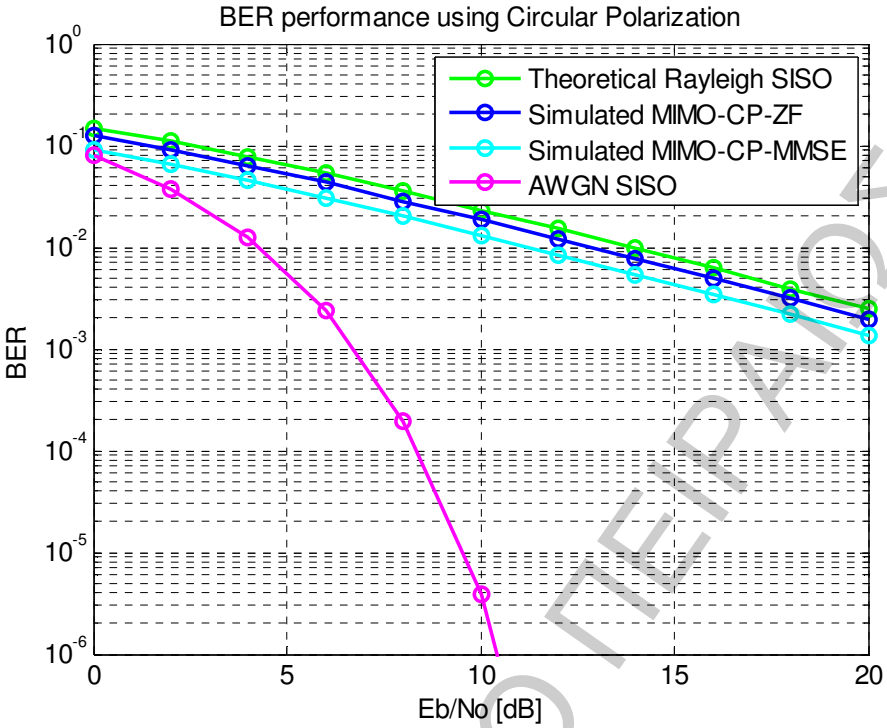

Figure 5-5: BER using CP

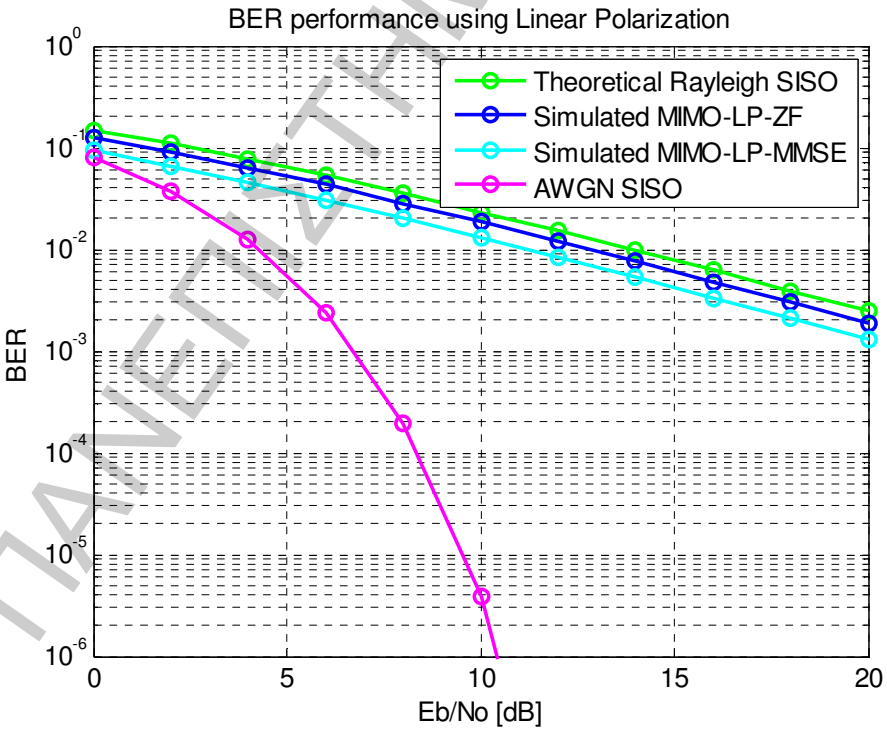

Figure 5-6: BER using LP

Also BER curves are shown in Figures 5-7 and 5-8, to illustrate the results obtained from simulating SIC ZF and SIC MMSE. As it is mentioned in the corresponding legends, the blue line represents the former case and the cyan line the latter case.

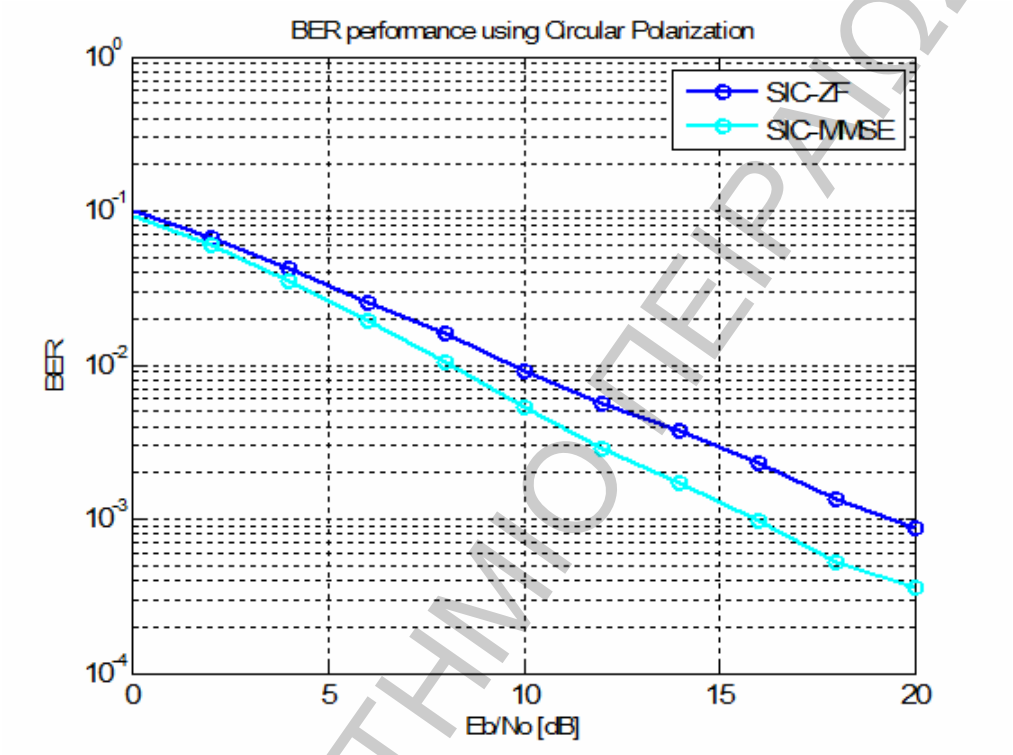

Figure 5-7: BER using SIC detection with CP

Observing Figures 5-7 and 5-8 circular and linear polarization has the same effect on the BER performance.

The most important parameter to explore when a communication system implements polarization techniques is the XPD. Figure 5-9, 5-10 and 5-11 present the XPD values for the antenna (XPD_{ant}) and for the environment (XPC_{env}) and also, the corresponding mean values in each case. The environement's XPC is constant as it is not affected from the large scale fading component, whereas the antenna's XPD – dependent on the large and small scale fading- changes in example, from intermediate tree shadow (Figure 5-9 using CP and 5-10 using LP) to heavy tree shadow (Figure 5-11) in this particular case.

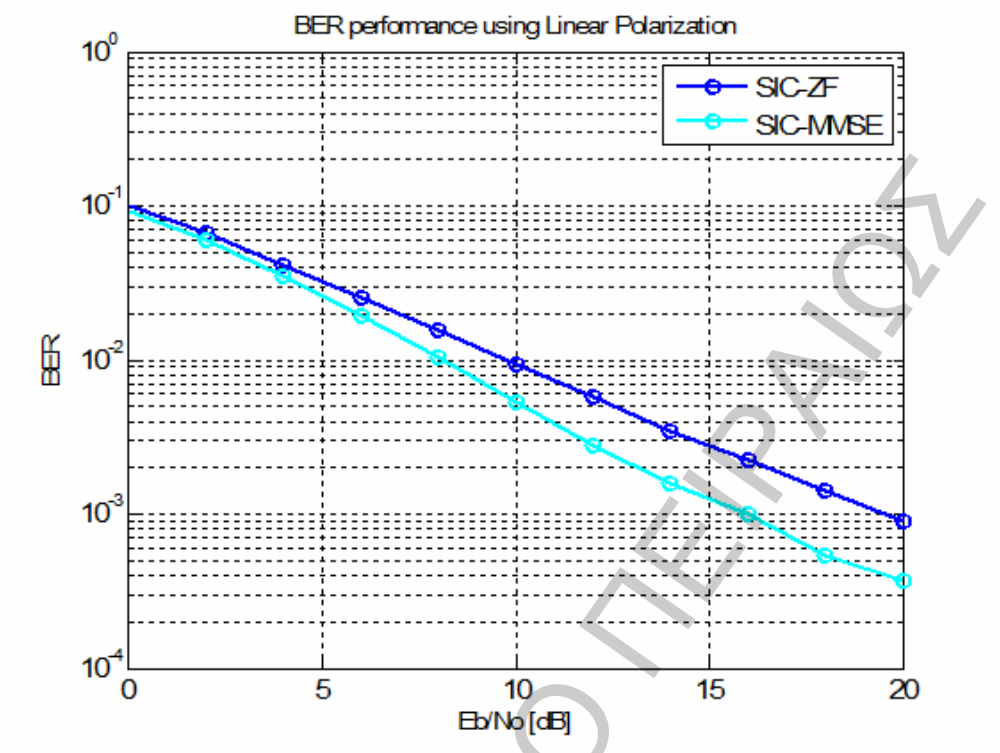

Figure 5-8: BER using SIC detection with LP

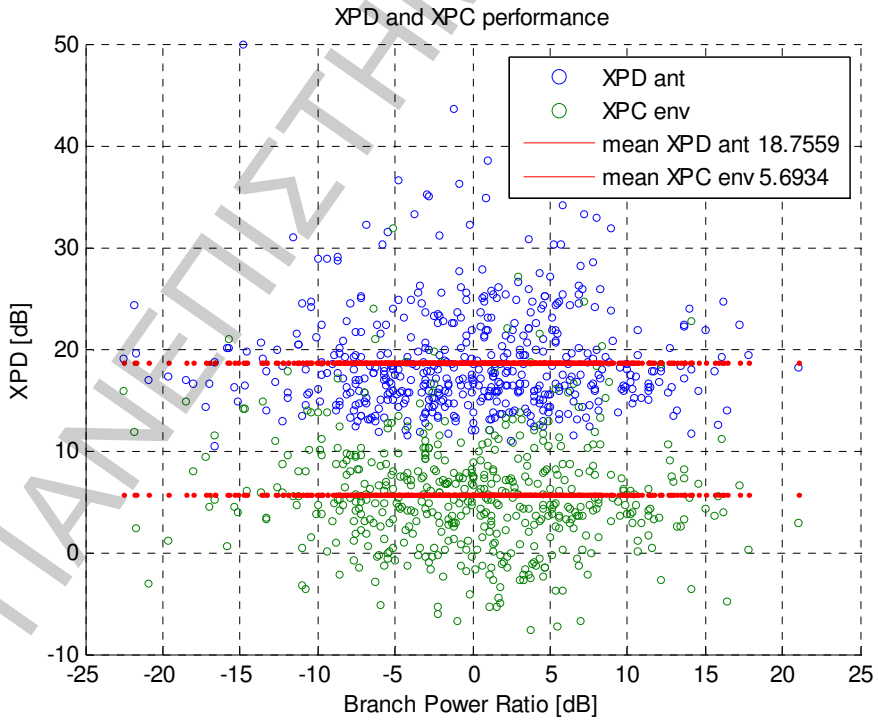

Figure 5-9: XPD for Intermediate Tree shadow env. using CP (S-band, 40° el. angle)

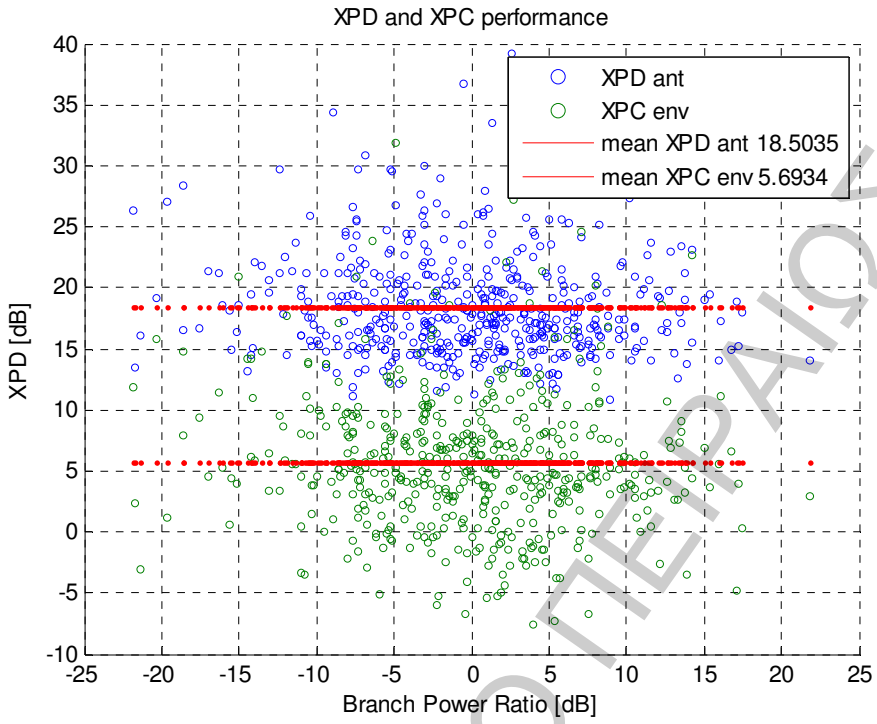

Figure 5-10: XPD for Intermediate Tree shadow env. using LP (S-band, 40° el. angle)

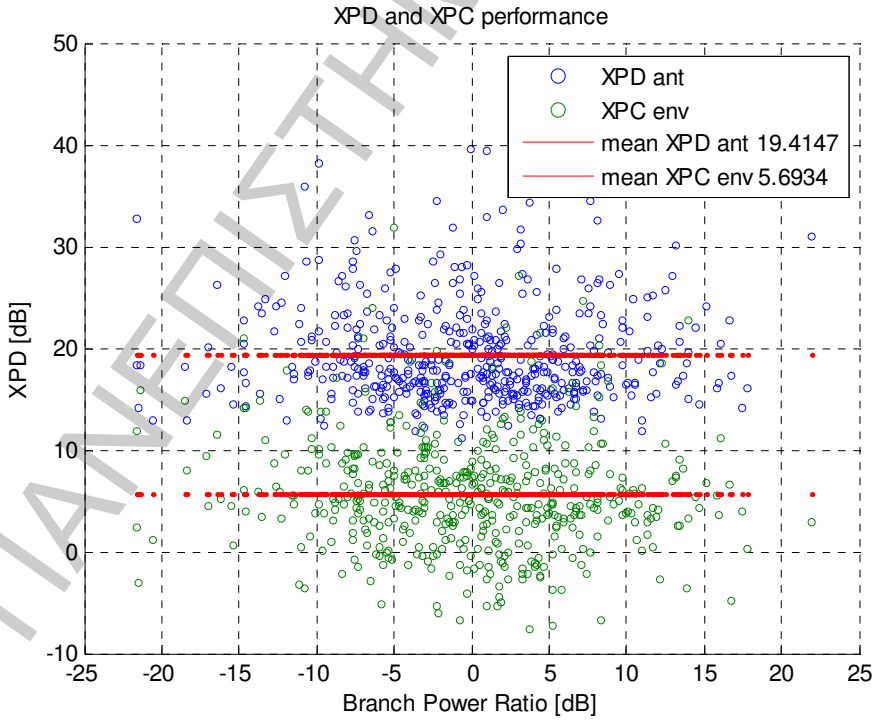

Figure 5-11: XPD for heavy tree shadow env. using CP (S-band, 80° el. angle)

Figures 5-9 to 5-11 show how the XPD values are distributed depending on the BPR. The first two figures may seem identical but actually they are produced using CP (the first diagram) and LP (the second diagram). The red lines represent the mean values of XPD_{ant} and XPC_{env} correspondingly. As expected from the similarity of the BER curves produced from CP and LP (Figures 5-5 and 5-6, 5-7 and 5-8), the mean XPC_{env} showing in Figures 5-9 and 5-10 is the same. A small difference is observed when it comes to the XPD_{ant} due to the channel's randomness.

To complete the report for the system performance, capacity results are obtained. The MIMO channel capacity depends on the antenna correlation. Although the capacity is not affected neither by the environment nor by the type of polarization used directly, the polarization diversity can eliminate the correlation effect and as a result, the capacity can be improved. Figure 5-12 shows the measured ergodic capacity for the SISO and the MIMO case for the two receivers where circular polarization is used.

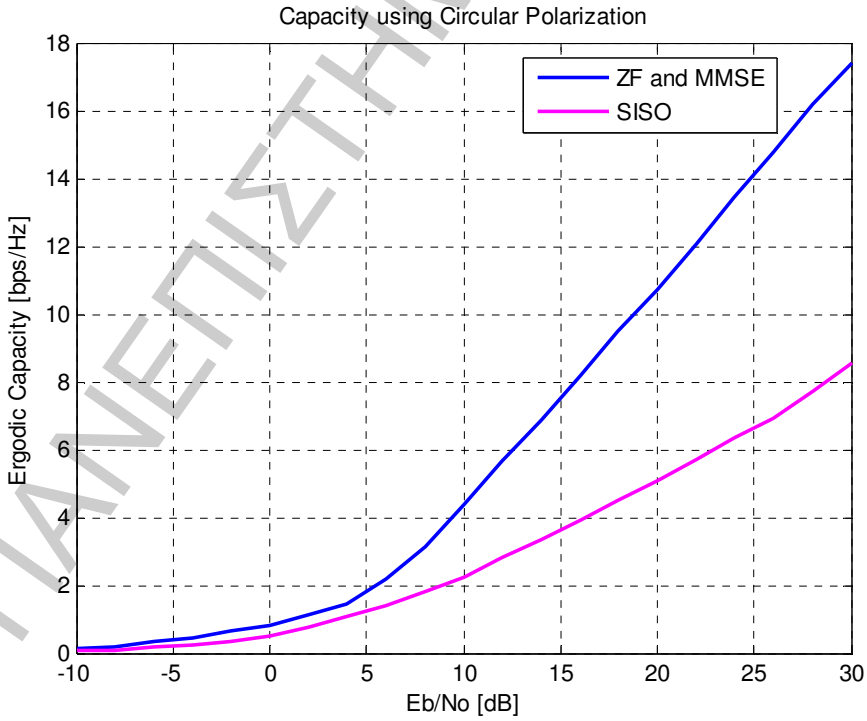

Figure 5-12: Capacity values for SISO and MIMO cases

References

[1] B. Evans, M. Werner, E. Lutz, M. Bousquet, G. E. Corazza, G. Maral, and R. Rumeau, "Integration of satellite and terrestrial systems in future multimedia communications," *IEEE Wireless Commun*., vol. 12, no. 5, pp. 72-80, Oct. 2005.

[2] R. Giuliano, M. Luglio, and F. Mazzenga, "Interoperability between WiMAX and Broadband Mobile Space Networks," *IEEE* Comm. Mag., vol. 46, no. 3, pp. 50-57, Mar. 2008.

[3] Evans, J.V.: "Satellite systems for personal communications", Proceedings of the IEEE, vol.86, no.7, 1998, pp.1325-1341

[4] Foschini, G. J. and M. J. Gans, "On limits of wireless communications in a fading environment when using multiple antennas," *Wireless Personal Communications*, vol. 6, no. 3, pp. 311-335, 1998.

[5] A. J. Paulraj, D.A. Gore, R.U. Nabar, and H. Bolcskei, "An overview of MIMO communications - A key to gigabit wireless," in *Proc. IEEE*, vol. 92, no. 2, pp. 198-218, 2004.

[6] P.-D. Arapoglou, K. Liolis, M. Bertinelli, A. Panagopoulos, P. Cottis, and R. De Gaudenzi, "MIMO over satellite: A review," *IEEE Commun. Surveys Tutorials*, vol. 13, no. 1, pp. 27-51, 2011.

[7] P.-D. Arapoglou, E. T. Michailidis, A. D. Panagopoulos, A. G. Kanatas, and R. Prieto-Cerdeira, "The Land Mobile Earth-Space Channel: SISO to MIMO Modeling from L- to Ka-Bands," *IEEE Vehicular Technology Magazine, Special Issue on Trends in Mobile Radio Channels: Modeling, Analysis, and Simulation*, vol. 6, no. 2, pp. 44-53, Jun. 2011.

[8] ETSI EM 302 583, "Digital Video Broadcast (DVB); Framing Structure, Channel Coding and Modulation for Satellite Services to Handheld Devices (SH) below 3 GHz," 2007.

[9] A. Bolea Alamanac, P. Burzigotti, R. De Gaudenzi, G. Liva, H. Nghia Pham, and S. Scalise, "In-depth analysis of the satellite component of DVB-SH: Scenarios, system dimensioning, simulations and field trial results," *Int. J. Satell. Commun. Networking*, vol. 27, no. 4-5, pp. 215-240, 2009.

[10] J. Goldhirsh and W. J. Vogel, "Mobile satellite systems fade statistics for shadowing and multipath from roadside trees at UHF and L-band," *IEEE Trans. Antennas Propagat*., vol. 37, no. 4, pp. 489-498, 1989.

[11] J. Dutronc and J. N. Colcy, "Land mobile communications in Kuband. Results of a test campaign on eutelsat I-F1," *Int. J. Satell. Commun*., vol. 8, no. 1, pp. 43-63, 1990.

[12] E. Lutz, D. Cygan, M. Dippold, F. Dolainsky, and W. Papke, "The land mobile satellite communications channel - Recording, statistics, and channel model," *IEEE Trans. Veh. Technol*, vol. 40, no. 2, pp. 375-386, 1991.

[13] A. Benarroch and L. Mercader, "Signal statistics obtained from a LMSS experiment in Europe with the Marecs satellite," *IEEE Trans. Commun*, vol. 42, no. 2/3/4, pp. 1264-1269, 1994.

[14] A. G. Kanatas and P. Constantinou, "City center high elevation angle propagation measurements at L-band for land-mobile satellite systems," *IEEE Trans. Veh. Technol*, vol. 47, no. 4, pp. 1002-1011, 1998.

[15] E. Kubista, F. Perez-Fontan, M. A. Vazquez-Castro, S. Buonomo, B. Arbesser-Rastburg, and J. P. Poiares Baptista, "Ka-band propagation measurements and statistics for land mobile satellite applications," *IEEE Trans. Veh. Technol*, vol. 49, no. 3, pp. 973-983, 2000.

[16] F. Pérez-Fontán, M. Vázquez-Castro, C. E. Cabado, J. P. Garcia, and E. Cubista, "Statistical modeling of the LMS channel," *IEEE Trans. Veh. Technol*., vol. 50, no. 6, pp. 1549-1567, 2001.

[17] S. Scalise, H. Ernst, and G. Harles, "Measurement and Modeling of the Land Mobile Satellite Channel at Ku-Band," *IEEE Trans. Veh. Technol*, vol. 57, no. 2, pp. 693-703, Mar. 2008.

[18] Claude Oestges and Bruno Clerckx, "MIMO Wireless Communications: From Real-World Propagation to Space-Time Code Design", April 2007

[19] P.R.King, "Modelling and Measurement of the Land Mobile Satellite MIMO Radio Propagation Channel" Ph.D. dissertation, University of Surrey, UK, June 2007.

[20] Francois Quitin, "Channel Modeling for Polarized MIMO Systems", Ph.D. dissertation, University of Louvain, France, June 2011.

[21] S. N. Livieratos and P. G. Corns, "Availability and performance of single/multiple site diversity satellite systems under rain fades," *Eur. Trans. Telecomm*., vol. 12, no. 1, pp. 55-65, Jan.-Feb. 2001.

[22] A. D. Panagopoulos, P. M. Arapoglou, and P. G. Cottis "Site vs. Orbital Diversity: Performance Comparison based on Propagation Characteristics at Ku band and above", *IEEE Anten. and Wirel. Propag. Letters*, vol. 23, no. 3, pp. 26-29, 2004.

[23] C. Nagaraja and I. E. Otung, "Statistical Prediction of Site Diversity Gain on Earth-Space Paths Based on Radar Measurements in the UK," *IEEE Trans. on Anten. and Propag*., vol. 60, no. 1, pp. 247-256, Jan. 2012.

[24] S. R. Saunders and A. A. Aragón-Zavala, *Antennas and Propagation for Wireless Communications*, 2nd ed. London, U.K.: Wiley, 2007.

[25] P. R. King and S. Stavrou, "Capacity Improvement for a Land Mobile Single Satellite MIMO System," *IEEE Anten. and Wirel. Propag. Let.*, vol. 5, no. 1, pp. 98-100, Dec. 2006.

[26] P. R. King and S. Stavrou, "Low Elevation Wideband Land Mobile Satellite MIMO Channel Characteristics," *IEEE Trans. on Wirel. Commun.*, vol. 6, no. 7, pp. 2712-2720, Jul. 2007.

[27] P. Horvath, G. K. Karagiannidis, P. R. King, S. Stavrou, and I. Frigyes, "Investigations in satellite MIMO channel modeling: Accent on polarization," *EURASIP J. Wireless Commun. and Networking: Special Issue on Satellite Communications*, no. 98944, 2007.

[28] P.-D. Arapoglou, M. Zamkotsian, and P. Cottis, "Dual polarization MIMO in LMS broadcasting systems: Possible benefits and challenges," *Int. J. Satell. Commun. Networking*, 2010.

[29] M. F. B. Mansor, T. W. C. Brown, and B. G. Evans, "Satellite MIMO Measurement With Colocated Quadrifilar Helix Antennas at the Receiver Terminal," *IEEE Anten. and Wirel. Propag. Letters*, vol. 9, pp. 712-715, 2010.

[30] E. Eberlein, F. Burkhardt, C. Wagner, A. Heuberger, D. Arndt, and R. Prieto-Cerdeira, "Statistical evaluation of the MIMO gain for LMS channels," in *Proc. 5th European Conference on Antennas and Propagation (EUCAP) 2011*, pp. 2695-2699, 11-15 Apr. 2011.

[31] D. Arndt, A. Ihlow, A. Heuberger, and E. Eberlein, "Antenna diversity for mobile satellite applications: Performance evaluation based on measurements," in *Proc. 5th European Conference on Antennas and Propagation (EUCAP)* 2011, pp.3729-3733, 11-15 Apr. 2011.

[32] T. W. C. Brown and A. Kyrgiazos, "On the small scale modelling aspects of dual circular polarised land mobile satellite MIMO channels in line of sight and in vehicles," in *Proc. 5th European Conference on Antennas and Propagation (EUCAP)* 2011, pp. 3562-3565, 11-15 Apr. 2011.

[33] P. R. King and S. Stavrou, "Land mobile-satellite MIMO capacity predictions," *Electron. Lett*., vol. 41, pp. 749-750, 2005.

[34] F. Yamashita, K. Kobayashi, M. Ueba, and M. Umehira, "Broadband multiple satellite MIMO system," in *Proc. 62nd IEEE Veh. Techn. Conf. (VTC) 2005*, vol. 4, pp. 2632-2636, Sep. 2005.

[35] P. R. King and S. Stavrou, "Characteristics of the Land Mobile Satellite MIMO Channel," in *Proc. IEEE 64th Vehicular Technology Conference (VTC-Fall) 2006*, pp.1-4, 25-28 Sep. 2006.

[36] K. P. Liolis, A.D. Panagopoulos, P.G. Cottis, "Multi-satellite MIMO communications at Ku-band and above: Investigations on spatial multiplexing for capacity improvement and selection diversity for interference mitigation," *EURASIP J. Wirel. Commun. Netw*., vol. 2007, Article ID 59608, 11 pages, 2007.

[37] B. N. Getu and J. B. Andersen, "The MIMO cube - a compact MIMO antenna," *IEEE Trans. on Wirel. Commun.*, vol. 4, no. 3, pp. 1136-1141, 2005.

[38] P.-D. Arapoglou, P. Burzigotti, M. Bertinelli, A. B. Alamanac, and R. De Gaudenzi, "To MIMO or Not To MIMO in Mobile Satellite Broadcasting Systems," *IEEE Transactions on Wireless Communications*, vol. 10, no. 9, pp. 2807-2811, Sep. 2011.

[39] Thomas A.Millign, "Modern Antenna Design", second edition, a John Wiley & Sons, inc., publication, 2005

[40] Watson P.A. and M Arbadi, "Cross Polarization Isolation and Discrimination", Electronics letter, vol.9, N.22, 1973

[41] K. P. Liolis, A. D. Panagopoulos, and S. Scalise, "On the Combination of Tropospheric and Local Environment Propagation Effects for Mobile Satellite Systems Above 10 GHz," *IEEE Trans. on Vehicul. Technol.*, vol. 59, no. 3, pp. 1109-1120, Mar. 2010.

[42] P. Horvath, G. K. Karagiannidis, P. R. King, S. Stavrou, and I. Frigyes, "Investigations in satellite MIMO channel modeling: accent on polarization," EURASIP J. Wireless Commun. Netw., June 2007

[43] Fengula Li, "Performance Analysis of V-BLAST Detectors for the MIMO channel", Master Degree Project, Sweden, 06/2007

[44] David Tse, "Fundamentals of Wireless Communication", University of California, Berkeley Pramod Viswanath, University of Illinois, Urbana-Champaign, 10/2004

[45] R. P. Cerdeira, F. Pérez Fontán, P. Burzigotti, A. Bolea Alamañac, and I. Sanchez Lago, "Versatile two-state land mobile satellite channel model with first application to DVB-SH analysis," Int. J. Satell. Commun. Netw., DOI: 10.1002/sat.964, 2010.

[46] Asad Mehmood and Abbas Mohammed,"Characterisation and Channel Modelling for Satellite Communication Systems", Blekinge Institute of Technology, Sweden

[47] F. Perez Fontan and P. Marino Espineira, "Modeling the Wireless Propagation Channel: A simulation Approach with Matlab", University of Vigo, Spain.